SWELLING OF ELASTOMERS DUE TO SIMULTANEOUS DIFFUSION OF BIODIESEL AND MULTI-AXIAL LARGE STRAIN

OMID KAHBASI

RESEARCH PROJECT SUBMITTED IN PARTIAL
FULFILMENT OF THE REQUIREMENTS FOR THE
DEGREE OF MASTER OF ENGINEERING

FACULTY OF ENGINEERING
UNIVERSITY OF MALAYA
KUALA LUMPUR

2013

UNIVERSITY OF MALAYA

ORIGINAL LITERARY WORK DECLARATION

(I.C/Passport No: **R14195405**)

Name of Candidate: **OMID KAHBASI**

Name of Degree: **MASTER OF MATERIAL ENGINEERING AND TECHNOLOGY**

Title of Project Paper/Research Report/Dissertation/Thesis (“this Work”):

SWELLING OF ELASTOMERS DUE TO SIMULTANEOUS DIFFUSION OF BIODIESEL AND MULTI-AXIAL LARGE STRAIN

Field of Study: **RUBBER MATERIAL**

I do solemnly and sincerely declare that:

1) I am the sole author/writer of this Work;
2) This Work is original;
3) Any use of any work in which copyright exists was done by way of fair dealing and for permitted purposes and any excerpt or extract from, or reference to or reproduction of any copyright work has been disclosed expressly and sufficiently and the title of the Work and its authorship have been acknowledged in this Work;

4) I do not have any actual knowledge nor do I ought reasonably to know that the making of this work constitutes an infringement of any copyright work;

5) I hereby assign all and every rights in the copyright to this Work to the University of Malaya (“UM”), who henceforth shall be owner of the copyright in this Work and that any reproduction or use in any form or by any means whatsoever is prohibited without the written consent of UM having been first had and obtained;

6) I am fully aware that if in the course of making this Work I have infringed any copyright whether intentionally or otherwise, I may be subject to legal action or any other action as may be determined by UM.

Candidate’s Signature Date

Subscribed and solemnly declared before,

Witness’s Signature Date

Name: Designation:

ABSTRACT

The concerns on depletion of petroleum-based fuel motivate the use of palm biodiesel as an alternative source of energy. However, the particular chemical composition of palm biodiesel affects significantly the performance of engineering components, in particularly elastomeric components. In this context, at least two important aspects contribute to the degradation of the elastomeric parts in service: diffusion of aggressive liquids leading to swelling and fluctuating multiaxial mechanical loading leading to fatigue failure. Hence, it is essential to understand the interactions between the two phenomena for durability analysis of the component. The present study investigates the swelling of elastomers due to diffusion of palm biodiesel in the presence of multiaxial large deformation and investigation on creep behavior of swollen elastomers. For this purpose, new experimental device and specimen are developed. The device consists of a hollow diabolo elastomeric specimen attached to specially-designed circular metallic grips and plates such that immersion tests can be conducted while the specimens are simultaneously subjected to various mechanical loadings: simple tension, simple torsion and combined tension-torsion. Thus, diffusion of liquids takes place in the material which concurrently undergoes multiaxial large deformation. Two types of elastomers are investigated: Nitrile Rubber (NBR) and Polychloroprene Rubber (CR). The particular features of the device and specimen are discussed and perspectives for further improvement are drawn.

Keywords: Elastomer, palm biodiesel, swelling, multiaxial large strain, hydrostatic stress, creep, creep modulus

ABSTRAK

Kebimbangan terhadap kekurangan bahan api berasaskan petroleum mendorong penggunaan biodiesel sawit sebagai sumber tenaga alternatif. Walau bagaimanapun, komposisi kimia tertentu biodiesel sawit memberi kesan ketara prestasi komponen kejuruteraan, terutamanya dalam komponen elastomer. Dalam konteks ini, sekurang-kurangnya dua aspek penting menyumbang kepada kemerosotan bahagian elastomerik dalam perkhidmatan: penyebaran cecair yang agresif yang membawa kepada bengkak dan turun naik muaton mekanikal pelbagai paksi membawa kepada kegagalan keletihan. Oleh itu, ia adalah penting untuk memahami interaksi antara kedua-dua fenomena untuk analisis ketahanan komponen. Kajian ini menyiasat bengkak elastomer kerana penyebaran biodiesel sawit di hadapan ubah bentuk yang besar pelbagai paksi dan penyiasatan ke atas kelakuan rayapan bengkak elastomer. Bagi tujuan ini, peranti baru eksperimen dan spesimen dibangunkan. Peranti ini terdiri daripada lubang Diabolo spesimen elastomerik melekat direka khas genggaman bulat logam dan plat seperti yang ujian rendaman boleh dilakukan manakala spesimen yang sama tertakluk kepada pelbagai beban mekanikal: ketegangan mudah, kilasan mudah dan gabungan ketegangan-kilasan. Oleh itu, penyebaran cecair berlaku dalam bahan yang serentak mengalami ubah bentuk yang besar pelbagai paksi. Dua jenis elastomer disiasat: Nitril getah (NBR) dan Polychloroprene Getah (CR). Ciri-ciri tertentu peranti dan spesimen dibincangkan dan perspektif untuk penambahbaikan telah disediakan.

Kata-kata: Elastomer, biodiesel sawit, bengkak, tekanan besar, pelbagai paksi, tekanan hidrostatik, rayap, modulus rayapan

ACKNOWLEDGMENT

Foremost, I would like to express my sincere gratitude to my advisor DR. SR ANDRI ANDRIYANA for the continuous support of my research project, for his patience, motivation, enthusiasm, and immense knowledge. His guidance helped me in all the time of research and writing of this thesis. I could not have imagined having a better advisor and mentor for my study.

I would like to thank my parents for supporting me spiritually throughout my life, and my sincere friend Hamid Taheri for all their supports.

TABLE OF CONTENTS

LIST OF FIGURES

LIST OF TABLES

CHAPTER 1 INTRODUCTION

1.1 Research background

The overwhelming global population growth and rapid industrialization have drastically increased the demand for petroleum-based fuel. This strong dependence has major consequences to the environment since the use of petroleum-based fuel contributes significantly to the greenhouse effect. Thus, considerations from environmental, political and economic factors motivate researchers to develop novel and renewable energy sources in order to decrease the dependence on petroleum based fuel(Trakarnpruk and Porntangjitlikit, 2008). In this context, biofuel is gaining popularity. It is produced by the transesterification of animal fats or plant oil and by far is the most promising solution to the concern of fossil fuels depletion and environmental pollution(Dwivedi et al., 2011). However, the particular chemical composition of biofuel affects significantly the performance of engineering components in particularly elastomeric parts such as seals, gaskets, pipes and o-rings. Indeed, in the case of palm biodiesel, it is established that the contamination of palm biodiesel into elastomers reduces significantly their mechanical properties (Haseeb et al., 2011).

In engineering applications involving the contamination of potentially aggressive liquids such as palm biodiesel into elastomeric components, there are at least two important aspects which contribute to the degradation of the materials in service: diffusion of aggressive liquids leading to swelling and fluctuating multiaxial mechanical loading leading to fatigue failure. Indeed, the presence of solvent in the rubber matrix weakens the matrix and decreases its resistance to failure (Fukumori et al., 1990). Hence, the understanding of interactions between the two phenomena is an essential prerequisite for the durability analysis of such components. Swelling of elastomers had been extensively studied by Flory (1953).and Treloar (2005) who investigated the swelling of stress-free rubber in solvents. In the case of stressed rubber, it was found that the tensile stress increases the liquid uptake while opposite phenomenon is observed in the presence of compressive stress. Treloar (2005) attributed these phenomena to the hydrostatic part of the Cauchy stress in the materials. The author provided the same argument for the decrease in swelling of rubber cylinder undergoing simple torsion. According to the author, the introduction of simple torsion generates the compressive stress along radial direction of the cylinder and thus limits the liquid uptakes. Similar results were obtained by Loke et al. (1972). It is important to highlight that in these works, the authors considered the swelling of solid hyperelastic cylinder undergoing simple torsion with infinitesimal small twisting angles, i.e. only small strain problems were studied. The extensions to the large strain simple torsion or general multiaxial loading were not provided. Thus, the effect of multiaxial mechanical loading on the level of liquid uptake in elastomers is not established. The objective of the present work is to investigate the swelling of elastomers in the presence of multiaxial large strain and the alteration of the viscoelastic behavior of elastomer due to swelling, in particular creep behavior of swollen elastomers. For this purpose, simple experimental specimen and device are developed such that immersion tests can be conducted while the specimens are simultaneously subjected to various mechanical loadings: simple tension, simple torsion and combined tension-torsion.

1.2 Research objectives

Objectives of this study are:

1. Investigating the effect of mechanical loading on the swelling of elastomers in palm biodiesel
2. Investigating the viscoelastic behaviors of swollen elastomers

1.3 Organization of dissertation

Chapter 1 sets the objectives while in chapter 2 the fundamentals of palm biodiesel, elastomers (particularly CR and NBR), swelling and the viscoelastic behavior of elastomer were provided while chapter 3 provides the details on the experimental device and specimen and the applied tests procedures for tensile, cyclic and creep test. Results and discussions are presented in chapter 4 in three parts, first is the evaluation of the experimental device followed by discussion over the swelling and cyclic results and lastly the creep result. Conclusion and recommendation is given in chapter 5.

CHAPTER 2 LITERATURE REVIEW

2.1 Palm oil biodiesel

2.1.1 Sustainable energy

Sustainable energy, specifically renewable energy or green energy is an energy source which can be replenished, that is essentially inexhaustible. Sustainable sources of energy include solar, wind, water, biomass and geothermal. Non renewable energy sources include coal, oil and natural gas.

2.1.2 Bioenergy

Bioenergy is sustainable energy produced from biomass, which is a general term for the material remains of once living organisms. Biomass includes agricultural crops, wood and wood by-products, fast-growing trees and plants, and industrial wastes. Burning this biomass creates the heat and steam that spins electricity-making turbines. Alternatively, biomass can be gasified and the gas used to power a gas turbine. Bioenergy is a clean energy source that creates little or no net greenhouse emissions depending on the type of biomass and conversion technology used.

2.1.3 Biodiesel

Bio-diesel, an earth friendly choice of consumers and renewable sources of alternative fuel occupies a great volume of the world’s fuel sector it is one of the newly energy sources which in oil and fat industry have attracted a lot of attention nowadays. Biodiesel is considered as a technology breakthrough which can be a substitute for petroleum fuel diesel. Biodiesels are driven from different kind of vegetables and animal fats. (McCarthy et al., 2011)

Biofuel is a renewable energy source produced from natural (bio-based) materials, which can be used as a substitute for petroleum fuels. The most common biofuels, such as ethanol from corn, wheat or sugar beet and biodiesel from oil seeds, are produced from classic food crops that require high-quality agricultural land for growth. However, ethanol is a petrol additive/substitute that can be produced from plentiful, domestic, cellulosic biomass resources such as herbaceous and woody plants, agricultural and forestry residues, and a large portion of municipal and industrial solid waste streams. Production of ethanol from biomass is one way to reduce both the consumption of crude oil and environmental pollution. There is also a growing interest in the use of vegetable oils for making biodiesel, which is less polluting than conventional petroleum diesel fuel (Demirbas, 2009)

2.1.4 Palm Biodiesel

Palm oil wastes are the main biomass resources in Asian countries. Malaysia is the world’s second largest palm oil producer and largest exporter. It is stated that until June 2009, there had been 406 palm oil mills in Malaysia with a total capacity of 92.78 million tons of Fresh Fruit Bunches (FFB) per annum (Tan et al., 2010). In Malaysia and Indonesia, which is being the two main largest palm oil producing countries in the world, there were about 30 million tons and 8.2 million tons of solid palm oil wastes which are such as Empty Fruit Bunch (EFB), fiber and shell generated respectively in year 2000 (Tan et al., 2010).

Palm Kernel is obtained from palm fruitlet after the removal of the MESOCARP and shell. It can be divided into two categories which are Palm Kernel Cake (PKC) and

Palm Kernel Shell (PKS). Palm kernel cake is a by-product from the kernel extraction process. It is used as a raw material for animal feed, especially for cattle feed. The PKC is obtained from the palm fruit within two stages of oil extraction. The primary stage is implemented by extraction of the palm oil in the pericarp part of the crushed kernel of the fruit. PKC is produced after the oil extraction of crushed kernel and is considered as by-product which comprises of conventional mechanical screw press method and solvent extraction method which the solvent extracted type is resulted.

PKS is an energy intensive substance and most difficult waste to decompose. Palm kernel shell is the waste kernel shell from Crude Palm Oil (CPO) processing. Due to the characteristic of PKS with high heating value compared to other biomass fuels and in terms of recycled waste matter as fuel, PKS is used widely used as fuels to generate heat for boilers or furnace in industries such as in the manufacturing plant, factories, etc. At present, there are 110,550 tons of PKS available annually. With the heating value of palm kernel shell about 17.4MJ/Kg, it is widely used mainly in power generation industries due to high demand from population growth (Prasertsan and Prasertsan, 1996).

2.1.5 Biodiesel vs. diesel

Several studies have been conducted to compare the performances of bio-diesel and conventional diesel, according to McCarthy et al (2011) the general performance deteriorates by increasing the blend ratio (biodiesel/diesel). The toque of the machine drops by 5% and there is a rise of 7 – 10% on fuel consumption which shows the lower energy content of bio-diesel. From the environmental point of view, the bio-diesel blend emits less than 27% Carbon monoxides (CO) compare to petroleum diesel while the Carbon dioxides (CO2) emissions were found to be higher with 6% for bio-diesel.(McCarthy et al., 2011)

Table 2.1 Biodiesel vs. Diesel

constituents	Diesel	Biodiesel	Implication
Heavy materials	Low	High	Heavy materials are prone to thermal cracking in hot section in the engineering and may result in engine fouling
Olefins	Low	High	The presence of olefins leads to poor thermal stability, leading to coking and poor oxidative stability.
Oxygen	Low	High	The higher oxygen contents lowering the energy contents of the fuel blend and influences the injection and burning properties that lead to an increase in the emissions of nitrogen oxides.
Solvating and detergent power	Low	High	Biodiesel is readily absorb more water and suspend solids
Long and large molecules	Low	High	Large constituents result in higher cloud points, cold filter plugging and set the lower operability temperature of the biodiesel.

2.2 Elastomeric (Rubber) Material

Polymers based on their characteristics at elevated temperature as well as if they are crosslinked or not, can be categorized into thermosets and thermoplastics. If a polymer can withstand to elongate more than 200% it will be categorized as “elastomer”, Elastomers in general can be either thermosets or thermoplastics.

What prevent materials like metals to flow and bring high stiffness is the attraction between atoms and molecules and the crystalline configurations. The elastomeric materials, with amorphous structure and weak interactions between molecules therefore, have different structural features which lead to become flexible.(Strong, 2006)

2.2.1 Natural Rubber (NR)

Natural rubber is a highly crosslinked polymer under aliphatic thermoset elastomer group which are the most common elastomeric materials. Even though crosslinks attach the polymers molecules together, however, if the material is not highly crosslinked it can take the advantage of showing elastomeric movement.(Strong, 2006)

One of the most advantages of crosslinks which will later be discussed on this research is to enhance the creep behavior at elevated temperatures. Natural rubbers have a high tendency to be softened and alternatively creep will occur at high temperature, this problem has been solved by a process called vulcanization in which strengthening of the materials obtains by crosslinking or cure of elastomeric material (cooking crude NR with sulfur).(Strong, 2006)

NR is a coagulated product of the latex of the rubber tree (hevea brasiliensis). NR characterizes excellence compression set, good resilience and abrasion, high tensile strength, and good vibration dampening characteristics, but poor resistance to petroleum oils and poor ozone, UV resistance are the main disadvantages of NR in industrial applications.(Columbia Engineering Rubber, 2012)

Crude natural rubber is composed of polyisoperen, which appear as cis-polyisoperen while the synthesis one is composed of trans-polyisoperen. Cis and trans prefixes are referred to the geometric isomerism of the polymers and this case cis-configuration means that H and CH_3 are on the same side of the double bond and on the opposite side for trans-configuration.(Fried, 2003)

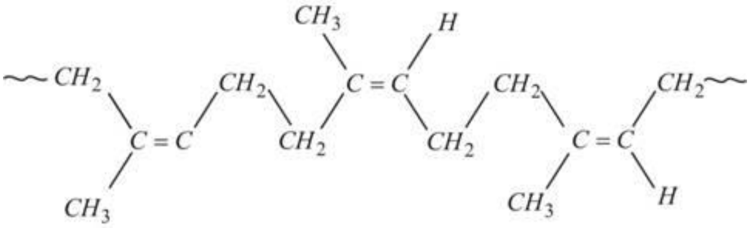

Figure 2.1 Cis-polyisoperen

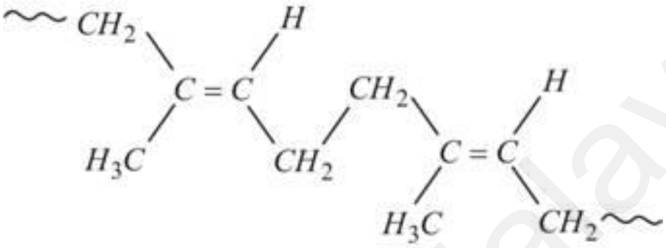

Figure 2.2 Trans-polyisoperen

The properties of these two configurations are different whereas the cis-configuration is the kind of natural rubber therefore heat sensitive and elastomeric while the trans-configuration is more hard because of having more interactions between the molecules.(Strong, 2006)

2.2.2 NBR rubber

Nitrile butadiene rubber (NBR) which used to be called Buna-N was developed to enhance oil resistant property which Natural Rubber (polybutadiene), lacks and now is one of the most widely used elastomer in the seal industry. Higher the content of nitrile is, more sensitivity to oil can be obtained. From chemistry point of view it is a family of unsaturated copolymers of acrylonitrile such as 2-propenenitrile and different kind of butadiene monomers such as 1,2-butadiene and 1,3-butadiene.(Strong, 2006)

Acrylonitrile is the product of the reaction between propylene and ammonia (Ram, 1997)

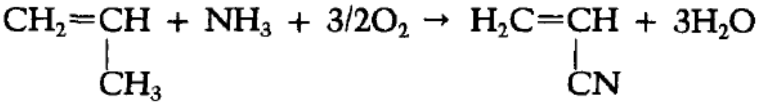

$$CH_2{=}\underset{\displaystyle CH_3}{\underset{|}{CH}} + NH_3 + 3/2O_2 \rightarrow H_2C{=}\underset{\displaystyle CN}{\underset{|}{CH}} + 3H_2O$$

Figure 2.3 Acrylonitrile production

The properties of NBR can be engineered by adjusting the content of acrylonitrile which its increase raises heat resistance as well as resistance to oils and fuels but decreases low temperature flexibility.(Columbia Engineering Rubber, 2012)

NBR carries good properties such as good abrasion resistance, improved resistance to degradation from oxidation but poor low temperature elasticity.

The higher price of NBR compare to both butadiene rubber and SBR limits its application where oil-resistance is needed. Typical application of NBR are in Oil resistant applications, Low temperature applications and oil and fuel systems for automotive, marine, and aircraft such as seals(O-rings, rubber seals), gaskets, conveyor belts.(Columbia Engineering Rubber, 2012, Strong, 2006)

2.2.3 CR rubber

Chloroprene (Neoprene®) is an oil-resistance polymer that was invented by DuPont in the 1930s. The molecular formula for chloroprene is C_4H_5Cl and the polymer structure is like polybutadiene with a chlorine bond to one of the carbon-carbon double bond. Big chlorine atoms in the chain cause intermolecular hindrance which turns the chloroprene into an oil-resistance and non-flammable rubber .(Strong, 2006)

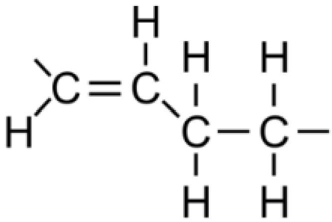

Figure 2.4 Polybutadiene chemical structure

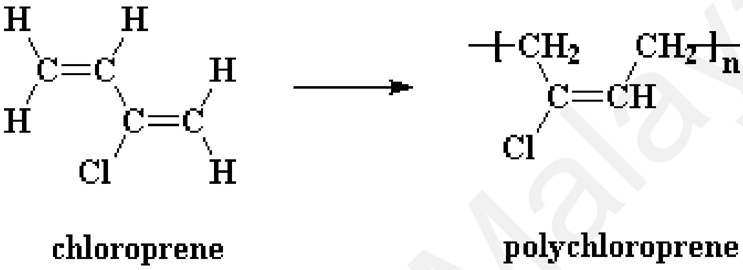

Figure 2.5 Chloroprene is a diene monomer, that is, it has two carbon-carbon double bonds

2.2.3.1 Properties:

Bing resistant to both oil and oxygen over a temperature range of -40F to +225F is one of the unique characteristics of chloroprene(SEALS, 2012). Neoprene is classified as a general purpose elastomer which has relatively low compression set, good resilience and abrasion, and is flex cracking resistant. Neoprene has excellent adhesion qualities to metals for rubber to metal bonding applications. It is used extensively for sealing refrigeration fluids due to its excellence resistance to Freon® and ammonia.(Columbia Engineering Rubber, 2012)

2.2.3.2 Application

O-rings, rubber seals and custom molded rubber components for refrigeration industry applications, general purpose seals, hose and wire (Columbia Engineering Rubber, 2012). Other applications of neoprene are fuel hoses, boots, shoe soles, and coating for fabrics where oil resistance and, perhaps, nonflammability are important. (Strong, 2006)

2.3 Swelling in Polymers

Many applications such as microlithography, biomedical devices, pharmaceutical and coatings involve swelling (Peters and Candau, 1988). In respect of swelling polymers can be divided into the water-swelling (cellulose, cotton, gelatin, wool, silk, wood, etc.) and the organic-liquid-swelling (the rubbers, both natural and synthetic) classes.

One of the best ways to model the swelling is the thermodynamic approach as swelling consists of phase; hence the free energy in this equilibrium should be a minimum by considering the changes in the swallowing rubber. The swelling of rubbers can be discussed by the mass changed or by the volume change (Flory, 1953), When a rubber is immersed in into a liquid, the liquid start penetrating into the polymer molecules which result to force apart the macromolecules which is consequently causes the reduction in strength and ductility due to breakage of the secondary bonding which give the viscoelastic characteristic to rubbers. The liquid penetration also lowers the glass transition temperature and. if depressed below the ambient temperature, will cause a once strong material to become rubbery and weak (Callister, 2007).

A number of important influential factors to swelling are how similar the structure of the polymer is to the chemical structure of the solvent, the temperature the molecular weight, the degree of crosslinking and crystallinity.

To investigate the thermodynamic behavior of selling we assume a case where there are two phases, one is liquid and the other phase is a solid with two components (mixed phase), hence this system free energy shall be a minimum with respect to changes in the composition of the mixed phase. Thus for the particular case when the mixed phase is polymer plus liquid and the single phase is the pure liquid, this means that the change in free energy resulting from the transfer of a small quantity of liquid from the pure liquid phase to the mixed phase shall be zero.

To represent this quantitatively it is convenient to introduce the Gibbs free energy of dilution L\Gt. defined as the change in the Gibbs free energy of the system due to the transfer of unit quantity (1 mol) of liquid (component 1) from the liquid phase to a very large quantity of the mixed phase. For a system at constant pressure the condition for equilibrium with respect to the transfer of liquid is then

$$\Delta G_1 = 0 \qquad (0.1)$$

The total free energy of dilution may be expressed in terms of the heat of dilution L\H1 and the entropy of dilution L\S1. Thus

$$\Delta G_1 = \Delta H_1 - T\Delta S_1 \qquad (0.2)$$

In this expression L\H1 and L\S1 are the corresponding changes in the heat content H and entropy S of the system per mole of liquid transferred from the liquid phase to the mixed phase. The heat content H is defined by the relation,

$$H = U + pV \qquad (0.3)$$

in which U is the internal energy and V the volume. When p is the atmospheric pressure, the effect of the term pV may generally be neglected, so that H and U become practically equivalent.

Experimentally, the derivation of ΔH_1 and ΔS_1 rests on the relation between these quantities and the equilibrium partial vapour pressures of the components in the mixed phase. In the case when only one component (the low-molecular-weight liquid) has an appreciable vapor pressure the molar free energy of dilution is given by

$$\Delta G_1 = RT\ln(p/p_0) \tag{0.4}$$

where p is the vapor pressure of the liquid component in equilibrium with the mixture (swollen rubber) at the temperature T and P0 is its saturation vapor pressure. (This equation assumes that the vapor obeys the perfect gas Jaws; if this assumption is not fulfilled a correction must be introduced.) The heat of dilution is thermodynamically related to the temperature dependence of relative vapor pressure,

$$\Delta G_1 = \frac{\partial(\Delta G_1/T)}{\partial(1/T)} = -RT^2\frac{\partial\ln(p/p_0)}{\partial(T)} \tag{0.5}$$

These two last Equations enable ΔG_1 and ΔH_1 to be determined by experiment; the remaining quantity ΔS_1 is then given by the difference between these two quantities by using Equation (0.2). (Treloar, 2005)

2.4 Mechanical response of elastomers

The mechanical properties and behavior of polymer materials particularly elastomers are different from metals and ceramics due to having different molecular structure consisting of chains with strong covalent bonds while individual chains are linked via secondary bonds (e.g., the van der Waals attractive forces). In such structure polymer chains slide over each other under stress and failure is the result of chain separation rather than breakage of interchain bonds. Thermosets are highly cross-linked and have brittle characteristics below glass transition temperature. Thermoplastics show varies of mechanical characteristics upon the degree of crosslinking and the content of stabilizers, fillers, or toughening agents. In contrast, even though rubbers are highly cross-linked but because of having a loose molecular network, they are capable of undergoing large deformations and return back to their original shape by releasing the stress. In elastomers, the amount of recoverable elastic strain can be 500% or more. (Liu, 2005)

For investigating the mechanical responses of rubbers different models have been developed considering the degree of incompressibility and viscoelastic behavior.

Choosing the right equations and models to describe material behavior is the most important part of modeling the material property and setting the proper calculations.

Here are the two models studied in this work:

1. Hyperelasticity: These models describe rubbers and foams, which can undergo shape changes but sustain reversible shape deformations.

2. Viscoelasticity: This model describes the materials that show a progressive increase when they go under a constant stress such as polymeric materials, polymer-based composites, and biological tissue (with stress rate-strain rate $\dot{\varepsilon} = \frac{\dot{\sigma}}{E} + \eta\sigma$ or that show hysteresis during cyclic loading (with stress rate-strain rate of form $\dot{\sigma} = E\varepsilon + \lambda\dot{\varepsilon}$).

2.4.1 Hyperelasticity

2.4.1.1 Continuum mechanics

Continuum mechanics was first developed by a French mathematician Augustin Louis Cauchy in 19th century. The continuum hypothesis is that many physical properties of materials, such as solids, liquids and gases, which are composed of molecules separated by empty space are perfectly continues in the microscopic scale (Roberts, 1994).

In continuum mechanics we mostly focus on a matter which goes under motion and deformation at the same time which makes it a four-dimensional space-time (kinematic) approach (Liu, 2002).

2.4.1.2 Elasticity

Elasticity is a physical property of materials in which the material returns to its original shape after being deformed. When an elastic material is subjected to an external force, internal forces induce inside the material which resist against the deformation and by removing the force they cause the material to return back to its original configuration (length, volume or shape). There are different elastic moduli, namely Young's modulus, the shear modulus, and the bulk modulus, all of which are measures of the strength of the restorative forces a material experiences.

For describing the elasticity of materials stress-strain curve is employed which shows the relation between stress (the average restorative internal force per unit area) and strain (the relative deformation).(Treloar, 2005)

When the stress-strain curve is linear as in most metals so the stress-strain relationship can be described by Hooke's law and higher-order terms will not get into account. But for elastomers and other rubber-like materials which are non-linearly elastic, isotropic, incompressible and generally independent of strain rate, by increasing the stress the slope of the stress-strain curve increases (Figure 2.6) which means the rubbers become harder to stretch, hence for rubbers Young’s modulus cannot be assigned to describe elasticity except for very small strains .(de With, 2006, Treloar, 2005)

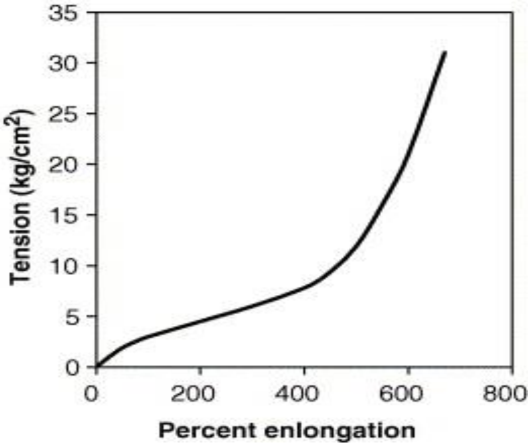

Figure 2.6 Rubbers' stress-strain curve

Hence for exploring the elasticity of elastomers Hyperelasticity model is used which is a **constitutive model** for an ideal elastic material in which the stress-strain relationship instead of the stress-strain curve, derives from a **strain energy density function**. The hyperelastic material is a special case of a **Cauchy elastic material**.(Ogden, 1997)

2.4.1.3 Displacement Gradient and Deformation Gradient Tensors

These quantities are defined by the following: Displacement gradient tensor: $\mathbf{u}\otimes\nabla$, is a tensor with components $\frac{\partial u_i}{\partial x_k}$ Deformation gradient tensor: $\mathbf{F}=\mathbf{I}+\mathbf{u}\otimes\nabla$ or in Cartesian components $F_{ik}=\delta_{ik}+\frac{\partial u_i}{\partial x_k}$

Where **I** is the identity tensor, with components described by the Kronecker delta symbol:

$$\delta_{ik}\begin{cases}1, i=k\\0, i\neq k\end{cases}$$

and ∇, represents the gradient operator. Formally, the gradient of a vector field u(x) is defined so that

$$[\mathbf{u} \otimes \nabla].n = \lim_{\alpha \to 0} \frac{u(x + \alpha n) - u(x)}{\alpha} \tag{0.6}$$

but in practice the component formula $\frac{\partial u_i}{\partial x_j}$ is more useful.

Note also that

$$\mathbf{y} \otimes \nabla = \big(x + u(x)\big) \otimes \nabla = \mathrm{F} \tag{0.7}$$

Or

$$\frac{\partial y_i}{\partial x_j} = \frac{\partial}{\partial x_j}(x_i + u_i) = (\delta_{ij} + \frac{\partial u_i}{\partial x_j}) = F_{ij} \tag{0.8}$$

The concepts of displacement gradient and deformation gradient are introduced to quantify the change in shape of infinitesimal line elements in a solid body. To see this, imagine drawing a straight line on the undeformed configuration of a solid, as shown in Figure 2.2. The line would be mapped to a smooth curve on the deformed configuration.

However, suppose we focus attention on a line segment dx, much shorter than the radius of curvature of this curve, as shown the segment would be straight in the undeformed configuration and would also be (almost) straight in the deformed configuration. Thus, no matter how complex a deformation we impose on a solid, infinitesimal line segments are merely stretched and rotated by a deformation. The infinitesimal line segments dx and dy are related by

$$dy = F.dx \quad or \quad dy_i = F_{ik} dx_k \tag{0.9}$$

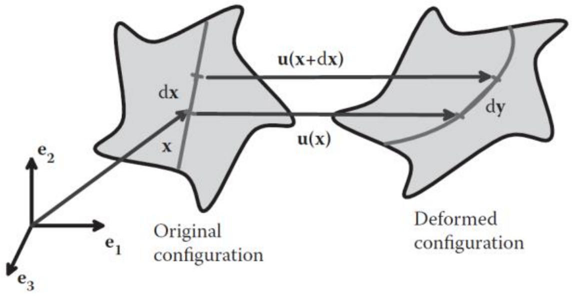

Figure 2.7 Deformation of an infinitesimal line element in a solid.

The inverse of the deformation gradient F^{-1}arises in many calculations. It is defined through (Bower, 2010)

$$dx_i = F_{ik}^{-1} dy_k \qquad (0.10)$$

2.4.1.4 Cauchy-Green deformation tensor

There are two Cauchy‐Green deformation tensors, defined through the following:

The right Cauchy‐Green deformation tensor:$C = F^T . F \quad C_{ij} = F_{ki} F_{kj}$

The left Cauchy‐Green deformation tensor:$B = F . F^T \quad B_{ij} = F_{ik} F_{jk}$

They are called “left” and “right” tensors because of their relation to the “left” and “right” stretch tensors defined below. They can be regarded as quantifying the squared length of infinitesimal fibers in the deformed configuration by noting that, if a material fiber $\boldsymbol{dx} = \boldsymbol{l_0 m}$ in the undeformed solid is stretched and rotated to $\boldsymbol{dy} = \boldsymbol{ln}$ in the deformed solid, then(Bower, 2010)

$$\frac{l^2}{l_0^2} = m . C . m \quad \frac{l_0^2}{l^2} = n . B^{-1} . n \qquad (0.11)$$

2.4.1.5 *Strain energy density function*

A **strain energy density function** or **stored energy density function** is a scalar valued function that relates the strain energy density of a material to the deformation gradient.

$$W = \hat{W}(C) = \hat{W}(F^T . F) = \bar{W}(F) = \bar{W}(B^{1/2} . R) = \tilde{W}(B, R) \qquad (0.12)$$

Equivalently,

$$W = \hat{W}(C) = \hat{W}(R^T . B . R) = \bar{W}(B^{1/2} . R) = \tilde{W}(B, R) \qquad (0.13)$$

Where F is the (two-point) deformation gradient tensor, C is the right Cauchy-Green deformation tensor, B is the left Cauchy-Green deformation tensor(Bower, 2010), and R is the rotation tensor from the polar decomposition of F.

For an anisotropic material, the strain energy density function $\hat{W}(C)$ depends implicitly on reference vectors or tensors (such as the initial orientation of fibers in a composite) that characterize internal material texture. The spatial representation $\tilde{W}(B, R)$ must further depend explicitly on the polar rotation tensor R to provide sufficient information to convert the reference texture vectors or tensors into the spatial configuration.

For an isotropic material, consideration of the principle of material frame indifference leads to the conclusion that the strain energy density function depends only on the invariants of C or, equivalently, the invariants of B since both have the same eigenvalues). In other words, the strain energy density function can be expressed uniquely in terms of the principal stretches or in terms of the invariants of the left Cauchy-Green deformation tensor or right Cauchy-Green deformation tensor and we have:

For isotropic materials,

$$W = \widehat{W}(\lambda_1, \lambda_2, \lambda_3) = \widetilde{W}(I_1, I_2, I_3) = \overline{W}(\bar{I}_1, \bar{I}_1.J) = U(I_1^c, I_2^c, I_3^c) \qquad (0.14)$$

with

$$\bar{I}_1 = J^{-2/3}I_1\ ; I_1 = \lambda_1^2 + \lambda_2^2 + \lambda_3^2\ ; J = \det(F) \qquad (0.15)$$

$$\bar{I}_2 = J^{-4/3}I_2\ ; I_2 = \lambda_1^2\lambda_2^2 + \lambda_2^2\lambda_3^2 + \lambda_3^2\lambda_1^2 \qquad (0.16)$$

A strain energy density function is used to define a hyperelastic material by postulating that the stress in the material can be obtained by taking the derivative of W with respect to the strain. For an isotropic, hyperelastic material the function relates the energy stored in an elastic material, and thus the stress-strain relationship, only to the three strain (elongation) components, thus disregarding the deformation history, heat dissipation, stress relaxation etc.

2.4.1.6 Strain Energy Density for Isotropic Solids

The following observations are the basis for defining the strain energy density of an elastic material:

If you deform a block of material, you do work on it (or, in some cases, it may do work on you).

In an elastic material, the work done during loading is stored as recoverable strain energy in the solid. If you unload the material, the specimen does work on you; when it reaches its initial configuration, you come out even.

The work done to deform a specimen depends only on the state of strain at the end of the test. It is independent of the history of loading.

Based on these observations, we define the strain energy density of a solid as the work done per unit volume to deform a material from a stress-free reference state to a loaded state.

To write down an expression for the strain energy density, it is convenient to separate the strain into two parts:

$$\varepsilon_{ij} = \varepsilon_{ij}^{e} + \varepsilon_{ij}^{T} \tag{0.17}$$

Where, for an isotropic solid,

$$\varepsilon_{ij}^{T} = \alpha \Delta T \delta_{ij} \tag{0.18}$$

Represents the strain attributable to thermal expansion (known as thermal strain), and

$$\varepsilon_{ij}^{e} = \frac{1+\upsilon}{E}\sigma_{ij} - \frac{\upsilon}{E}\sigma_{kk}\delta_{ij} \tag{0.19}$$

is the strain attributable to mechanical loading (known as elastic strain). Work is done on the specimen only during mechanical loading. It is straightforward to show that the strain energy density is

$$U = \frac{1}{2}\sigma_{ij}\varepsilon_{ij}^{e} \tag{0.20}$$

You can also rewrite this as

$$U = \frac{1+\upsilon}{2E}\sigma_{ij}\sigma_{ij} - \frac{\upsilon}{2E}\sigma_{kk}\sigma_{jj} \tag{0.21}$$

$$U = \frac{E}{2(1+\upsilon)}\varepsilon_{ij}^{e}\varepsilon_{ij}^{e} + \frac{E\upsilon}{2(1+\upsilon)(1-2\upsilon)}\varepsilon_{ij}^{e}\varepsilon_{kk}^{e} \tag{0.22}$$

Observe that

$$\varepsilon_{ij}^{e} = \frac{\partial \mathrm{U}}{\partial \sigma_{ij}}\sigma_{ij} = \frac{\partial \mathrm{U}}{\partial \varepsilon_{ij}^{e}} \tag{0.23}$$

2.4.1.7 Decomposition Into Hydrostatic And Pure Shear States

It will be shown in the present section that resolved into a hydrostatic state and a state referred to a coordinate system be an arbitrary state of stress can be of pure shear. Let the given state referred to a coordinate system be

$$[\tau_{ij}] = \begin{bmatrix} \sigma_x & \tau_{xy} & \tau_{xz} \\ \tau_{xy} & \sigma_y & \tau_{yz} \\ \tau_{xz} & \tau_{yz} & \sigma_z \end{bmatrix} \quad (0.24)$$

Let

$$p = \frac{1}{3}\left(\sigma_x + \sigma_y + \sigma_z\right) = I_1 \quad (0.25)$$

The given state can be resolved into two different states, as shown:

$$\begin{bmatrix} \sigma_x & \tau_{xy} & \tau_{xz} \\ \tau_{xy} & \sigma_y & \tau_{yz} \\ \tau_{xz} & \tau_{yz} & \sigma_z \end{bmatrix} = \begin{bmatrix} p & 0 & 0 \\ 0 & p & 0 \\ 0 & 0 & p \end{bmatrix} + \begin{bmatrix} \sigma_x - p & \tau_{xy} & \tau_{xz} \\ \tau_{xy} & \sigma_y - p & \tau_{yz} \\ \tau_{xz} & \tau_{yz} & \sigma_z - p \end{bmatrix} \quad (0.26)$$

The first state on the right-hand side of the above equation is a hydrostatic state.

The second state is a state of pure shear since the first invariant for this state is

$$\mathrm{I}_1' = (\sigma x - p) + (\sigma y - p) + (\sigma z - p) = \sigma x + \sigma y + \sigma z - 3p = 0 \quad (0.27)$$

1f the given state is referred to the principal axes, the decomposition into a hydro static state and a pure shear state can once again be done as above, i.e.

$$\begin{bmatrix} \sigma_1 & 0 & 0 \\ 0 & \sigma_2 & 0 \\ 0 & 0 & \sigma_3 \end{bmatrix} = \begin{bmatrix} p & 0 & 0 \\ 0 & p & 0 \\ 0 & 0 & p \end{bmatrix} + \begin{bmatrix} \sigma_1 - p & 0 & 0 \\ 0 & \sigma_2 - p & 0 \\ 0 & 0 & \sigma_3 - p \end{bmatrix} \quad (0.28)$$

Where, as before,

$$p = \tfrac{1}{3}\left(\sigma_x + \sigma_y + \sigma_z\right) = I_1. \quad (0.29)$$

The pure shear state of stress is also known as the deviatoric state of stress or simply as stress deviator.(Srinath, 2009)

2.4.2 Viscoelasticity

Many polymers shows a behavior which is neither pure elastic behavior nor exhibits pure viscose characteristic, this property is called viscoelasticity. When a viscoelastic polymer goes under stress, an immediate elastic response occurs which is followed by viscous flow. This flow decreases with time until it meets a stable state. By unloading the material, this elastic strain recovers immediately which is again followed by the recovering of the time-dependent viscose strain, which called delayed recovery. Even after unloading the material and giving enough time for the recovery there is still a permanent strain which is called permanent recovery. (Liu, 2005)

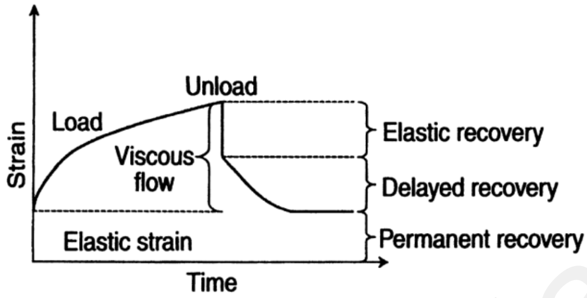

Figure 2.8 Viscose characteristic

2.4.2.1 Viscoelastic mechanical models

As it’s been discussed, there are two mechanical responses from viscoelastic materials, one is elastic behavior which is similar to an ideal spring response and the other one is viscose behavior and can be modeled by a dashpot which can be viewed as a shock absorber consisting of a piston in a cylinder which is filled with a fluid with the viscosity of η.

2.4.2.2 Maxwell Element

It represents a series combination of a spring and a dashpot; this model can be calculated by adding up the strain rate on the spring with the strain rate of the dashpot.

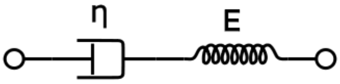

Figure 2.9 Maxwell element model

It should be noted that the strain and stress in the spring element are sinusoidal time-dependent functions with δ phase angle.

$$\frac{d\varepsilon}{dt} = \frac{d\varepsilon_{dashpot}}{dt} + \frac{d\varepsilon_{spring}}{dt} = \frac{\sigma}{\eta} + \left(\frac{1}{E}\right)\frac{d\sigma}{dt} \qquad (0.30)$$

A term τ (relaxation time) is defined later on as: $\tau = \frac{\eta}{E}$ applying this model for stress-relaxation, where strain is constant will reduce this equation to a first-order differential equation $\frac{d\sigma}{\sigma} = -\left(\frac{1}{\tau}\right)$ dt which the stress response can be given as $\sigma = \sigma_0 exp\left(\frac{-t}{\tau}\right)$

In creep test which a constant stress is applied, the second sentence will become zero and the equation will be deducted to $\frac{d\varepsilon}{dt} = \frac{\sigma_0}{\eta}$ which gives $\varepsilon(t) = \left(\frac{\sigma_0}{\eta}\right)t + \varepsilon_0$

The prediction of viscoelastic creep by the Maxwell model can be shown as

$\frac{D(t)}{D} = 1 + \frac{1}{\tau}$ (Fried, 2003)

2.4.2.3 Voigt Element

This model (sometimes called Kelvin model) is a parallel combination of a dashpot and a spring which exhibits a uniform strain in all the elements.

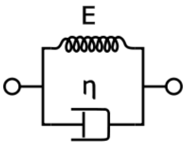

Figure 2.10 Voigt element model

$$\varepsilon = \varepsilon_1 = \varepsilon_2 \tag{0.31}$$

And the overall stress is the summation of stresses in each component

$$\sigma = \sigma_1 + \sigma_2 \tag{0.32}$$

Hence

$$\frac{d\varepsilon}{dt} = \frac{\sigma}{\eta} - \frac{\mathrm{E\varepsilon}}{\mathrm{\eta}} \tag{0.33}$$

This model is unsuccessful to give a good presentation of stress-relaxation in polymers because of having a constant strain which leads to linear elastic response $\sigma = E\varepsilon$

In the creep test the Voigt model gives a suitable response as by solving the equation it gives $\varepsilon = \frac{\sigma_0}{E}\left[1 - exp\left({}^{-t}/{}_{\tau_0}\right)\right]$ which shows how the strain rate decreases when t→∞. (Ram, 1997)

The prediction of viscoelastic creep by the Voigt model can be shown as(Fried, 2003)

$$\frac{D(t)}{D} = 1 - \exp\left(\frac{-1}{\tau}\right) \tag{0.34}$$

2.4.2.4 Multi-element model

In practice materials behave in a very complicated way compare to single Maxwell and Voigt model, these behaviors can be modeled as the combination of Maxwell and Voigt in parallel and in series.

There are two famous models which are the combination of Maxwell and Voigt. One is Maxwell-Wiechert model which is a combination of parallel Maxwell model elements and the second one is Voigt-Kelvin model in which there are series of Voigt elements.

Voigt-Kelvin model can describe the creep by considering N Voigt elements as (Fried, 2003)

$$D(t) = \sum_{i=0}^{N} D_i \left[1 - \exp\left(\frac{-1}{\tau}\right)\right] \tag{0.35}$$

CHAPTER 3 METHODOLOGY

This chapter covers the design of a novel test setup which impose multi-axial loading on rubbers and the procedures for the evaluation of creep phenomenon and stress relaxation in biodiesel-immersed rubbers.

On this work, two sets of test have been conducted with slightly different procedure in the sense of immersion. One is designed to use cyclic test for investigating of the swelling and mechanical responses of rubbers undergoing biodiesel immersion and multiaxial stresses and the second experiment deals with the creep responses of biodiesel-immersed rubbers.

In each sets two types of rubber, CR (Chloroprene) and NBR (Nitrile butadiene rubber), are used as they both are widely used in the industry but have different mechanical responses and oil absorption rate.

3.1 Design of the experimental device

In order to investigate the diffusion of palm biodiesel into elastomers undergoing multiaxial large strain, specially-designed specimen and device are developed. They consist of a hollow diabolo elastomeric specimen equipped with circular metallic grips and plates as shown in Figure 3.1and Figure 3.2. The main features of the device and specimen are summarized as follow:

3.1.1 Specimen

The rubber specimen has a diabolo-like shape with a hollow inside to allow the biodiesel to diffuse into the specimen from the inner and outer wall surfaces. Thus, equilibrium swelling can be achieved within a reasonable period of time. The middle part of the specimen is the part of investigation as it’s imposed to oil, the other two end of diabolo get into the grips which mostly makes the oil penetration to the inner part. Geometry of rubber specimen

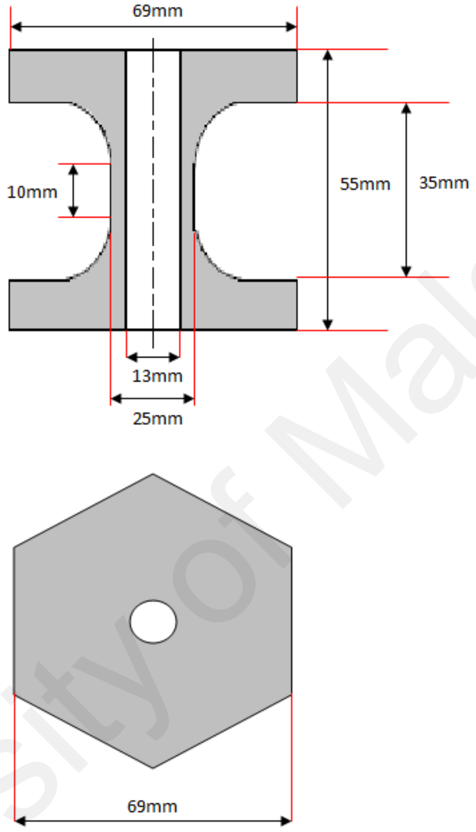

Figure 3.1 Test specimen(Ch’ng et al., 2013)

The middle part (under investigation part) has an inner diameter of 13mm and the outer diameter of 25mm which forms a cylinder with the wall thickness of 12mm and the length of 10mm Figure 3.1. The thickness and length have been chosen, considering twisting the specimen does not result in wrinkling.

The outer diameter of the cylinder increases by getting far from the center part in a curve shape in order to withstand any shape changes by the stresses (The stresses are meant to affect the middle part only).

Now this piece (the middle part and the curved conic shape parts) is ended to two hexagonal plates which are in charge of: 1- Their edges are fasten the specimen in the grips and prevent rotation while undergoes twist 2- the down part of the plate is designed to withstand the stresses due to tension in other word grips pull the hexagonal plates apart and they stretch the middle part (Ch’ng et al., 2013).

3.1.2 The metallic device

The device consists of four identical metallic grips which are screwed together at both ends of the elastomeric specimen. The inner part of the metallic grips is designed to fit in the hexagonal shape of the specimen. In this way, twist and axial extension/contraction can be imposed simultaneously to the specimen while the immersion test is carried out.

Each metallic grip consists of six identical holes located at the angle of 30 ° apart from each other. Different twist can be set to the specimen by twisting the upper part of metallic grip while fixing the lower part of the grip. Once the desired angle is chosen, bolts are inserted through the holes located at the lower and upper parts of the grip in order to maintain constant twist. Axial extension or contraction can be imposed by adjusting vertically the position of the nuts in the bolts as illustrated in Figure 3.3.

After the metallic grips are tightly screwed to the specimen, thin metallic plates are attached at both ends in order to prevent the diffusion of liquids from both specimen ends. Two o-rings with different diameter are inserted between plates and grips to provide a tight seal.(Ch’ng et al., 2013)

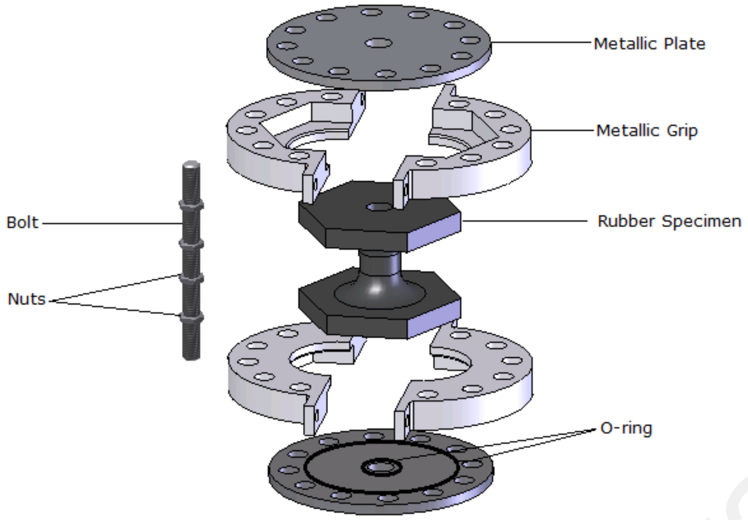

Figure 3.2 Exploded view of the experimental device and specimen.(Ch'ng et al., 2013)

3.2 Materials and experiment

3.2.1 Materials

Specially designed elastomers are purchased from MAKA Engineering Sdn. Bhd., Malaysia. The as-received elastomeric specimens investigated in this work are commercial grades of NBR and CR with 60 shore hardness and 25 wt% of carbon black content which were molded by using injection-molding. Palm biodiesel is provided by Mission Biotechnologies Sdn. Bhd. All immersion tests are conducted in 100 % palm biodiesel at room temperature.

3.2.2 Immersion procedure

3.2.2.1 For cyclic test (multiaxial loading)

As mentioned previously, our particular device and specimen allow the immersion test to be conducted on the specimens while they are subjected to different mechanical loading conditions. In the present study, eight different mechanical loading conditions are investigated. The details of these conditions are given in **Error! Reference source not found.**. An illustration of the specimen and device before and after the application of mechanical loading, i.e. tension and torsion, is provided in Figure 3.3.

Table 3.1 Specimens mechanical conditions (Ch'ng et al., 2013)

Specimen	Applied Load			
	Tensile Load		Torsional Load	
	Axial extension ΔL (mm)	Resulting stretch ratio λ = L/L0	Twist angle θ (°)	Resulting twist per unit length = θ/L (rad/mm)
S0 T0	0	0	0	0
S0 T30	0	0	30	0.02094
S0 T60	0	0	60	0.04189
S0 T90	0	0	90	0.06283
S20T0	5	1.2	0	0
S20T30	5	1.2	30	0.01745
S20T60	5	1.2	60	0.03491
S20T90	5	1.2	90	0.05236

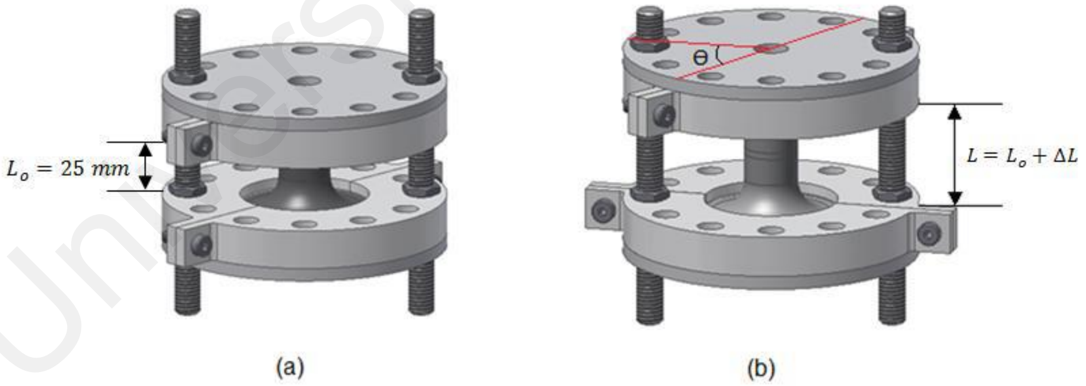

Figure 3.3 Experimental device: (a) with no mechanical loading (stress-free) and (b) under twist angle and axial extension ΔL.(Ch'ng et al., 2013)

After the desired axial extension (ΔL) and twist angle (θ) have been applied, the specimens are completely immersed in palm biodiesel for one week. In order to determine the swelling level, the mass of the specimens before and after immersion test is measured. The detailed procedures of immersion test can be summarized as follow:

1. Before immersion test, the mass of the dry rubber specimen is measured using digital weighting machine.

2. The rubber specimen is subsequently attached into the experimental device as described in the previous section in order to impose the mechanical loading.

3. The experimental devices are then immersed into palm biodiesel for one week at room temperature.

4. After one week, the devices are removed from the biodiesel and the rubber specimens are dismantled from the metallic plates and grips. The specimens are then quickly dipped into acetone and cleaned with filter paper to remove excessive oil.

5. The mass of the specimens after immersion is measured as in step 1. The percentage of mass change is calculated using the following simple relation:

$$\%\ \text{Mass Change} = \frac{M_2 - M_1}{M_1} \times 100$$

Equation Chapter 3 Section 1

(3.1)

Where M1 and M2 are the masses of the specimen before and after immersion respectively.

3.2.2.2 For creep test

For the creep test twenty NBR specimens and twenty CR specimens are allocated in groups of four, the first groups (NBR and CR) goes under test in a dry state while the second, third fourth and fifth are immersed in the palm oil biodiesel in stress-free state for one, two, three and four weeks respectively to get prepared for tensile and creep test. Before doing the creep test we need to determine the swelling level.

1. A digital weighting machine is used to measure the mass of the dry rubber specimens before the immersion.

2. The rubber specimens are put in stainless steel containers which are filled with palm oil biodiesel.

3. The first groups are not immersed while the second, third fourth and fifth are immersed for one, two, three and four weeks respectively.

4. Removing the specimens out of oil is followed by an instant immersion in acetone for 5 seconds which removes the surface excessive oil.

5. As it’s been mentioned the percentage of mass change is calculated by (3.1).

3.3 Mechanical testing

3.3.1 Tensile test

ASTM provides the procedures for evaluating the tensile (tension) properties of vulcanized thermoset rubbers and thermoplastic elastomers. Specimens can be in the shape of dumbbells, rings or straight pieces of uniform cross-sectional area. It should be noted that the specimen shouldn’t have been prestressed before as the tensile strength is based on the original cross-sectional area. (ASTM.D412, 1998)

3.3.1.1 Experimental procedure

- Measuring the inner diameter (the hollow diameter),D_i and the outer diameter D_o which is the center of the diabolo (using the vernier caliper) after Immersion.
- Calculating the initial cross-section area by $A = \frac{\pi}{4}(D_o^2 - D_i^2)$ and the initial length, l_0 by measuring the distance between the inner sides of the two grips.

- Fitting the specimen in the grips and attaching the tensile test caps (the metallic grip with a handle to fit in the tensile apparatus) on the grip and place the whole set on the tensile machine.
- Set the speed of extension to 1mm/s and insert the initial cross-section area and length to the machine.
- Performing the test till failure.

3.3.2 Cyclic test

This test method is based on the measuring of the extension as a function of the time of a test sample subject to tensile load. The cyclic tensile test shows a number of well-known phenomenon in rubbers, referred as the Mullins effect(Mullins, 1948). The path of stress – strain diagrams differs significantly when loading to unloading which creates a hysteresis diagram and the calculated energy between the paths refers to hysteresis of energy. When the specimen is unloaded at the point where there is no force the length of the specimen is longer than the initial length, this refers to as the residual strain. The stress at each cycle decreases compare to a cycle before even though the process is strain-controlled (the maximum strain per cycle is fixed) this phenomenon is called strain-softening, but after a number of cycles of loading – unloading the changes in stress wouldn’t be noticeable. . When stretching of a sample proceeds after several cycles, the stress – strain curve rapidly reaches that for a virgin specimen under the same loading conditions (strain-hardening).

Chagnon and Verron describe the formation of hysteresis of energy when a rubber goes under cyclic loading as the breakage and restoration of links and bonds between polymer chains and between the matrix and aggregates of filler.(Chagnon et al., 2006)

There is a method known as accounting for damage which describes the strain-softening of a rubber which undergoes cyclic test.(Govindjee and Simo, 1992)

3.3.2.1 Experimental procedure

Cyclic test takes the same steps as the tensile test and the parameters such as cross-section area, initial length, speed, number of cycles and maximum tensile strain (200%) are needed to be inserted.

Dumbbell specimens for cyclic tests are as same as the ones for uniaxial tensile test with the ring-like cross-sectional area **Error! Reference source not found.**. Mechanical tests were performed at ambient temperature by using a universal testing machine Instron. There is a load cell on the machine which measures the tensile force and the Instron program determines the stress σ as the ratio of axial force to cross-sectional area of specimens in the stress-free state. The strain rate set to $\dot{\epsilon} = 6 \times 10^{-2}\ s^{-1}$ and the specimens were stretched up to strain $\epsilon_{max} = 2$ with the $\dot{\epsilon}$, followed by unloading with the $-\dot{\epsilon}$ rate to zero stress where there is no force but the grips are further from each other compare to the start of the test as the specimen elongates after the first loading (residual strain). The second reloading is then instantly performed to the ϵ_{max} followed by unloading. This cycle need to be repeated until the loss moduli and storage moduli get fix in the cycle.

3.3.3 Creep test

Plastics inherently respond differently to mechanical loads from metals and ceramics. When it comes to creep while a rubber plastic goes under a constant load the strain can be derived from the stress-strain modulus, and then the deformation continues in a slower manner until it fails. This phenomenon is what is known as creep. Creep behavior depends on four known factors, the type of plastic, amplitude of load, atmosphere's temperature and time. Creep is a time dependence phenomena which restricts the use of stress-strain data in designing.(O'Toole, 1968)

The general creep test is plotted the strain percentage over time, as it can be seen the Figure 3.4 the curve can be divided into 4 continue stages. The first stage (instantaneous deformation) is the instantaneous strain at the beginning of the test followed by the second stage (primary) in which strain occurs fast but the rate of the strain is decreasing, on the third stage (secondary) the rate remains constant up to a point when on the fourth stage (tertiary) both the speed and rate of strain increase until the test sample fails.(Delatycki, 1971)

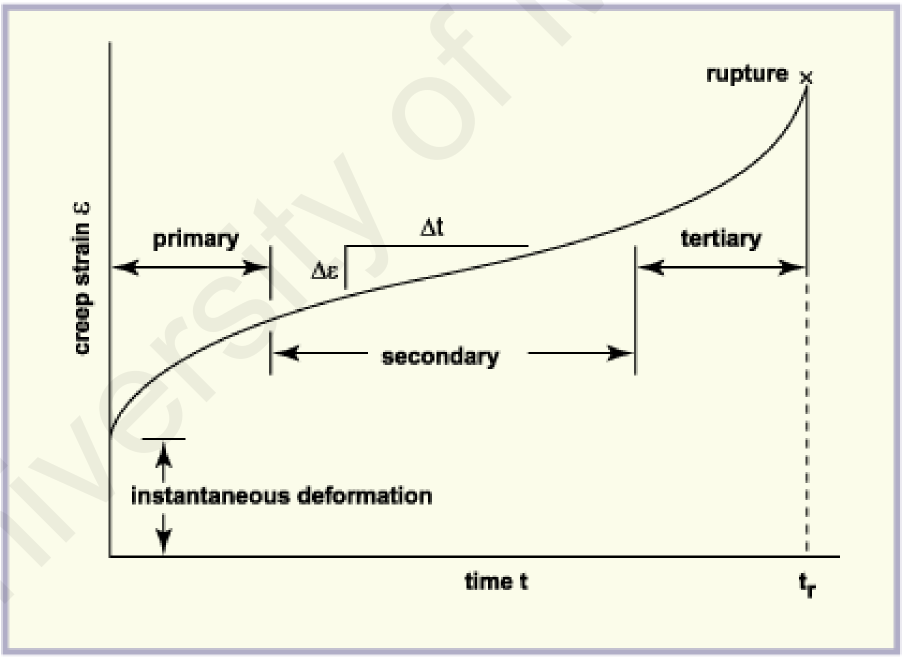

Figure 3.4 Creep curve diagram

3.3.3.1 Creep Tests

This work is more on finding a right method and calculation of creep data in order to find the most realistic comparable results. Creep test in polymer rubber can be evaluated by two methods, one is Tensile Creep, which described in ASTM D 2990 and ISO 899-1 and the other one is Flexure Creep (ASTM D 790, ISO 6602). In tensile creep the test sample goes under a constant load, by making a two-gauge mark, the extension can be measured at time intervals. Dividing the extension by the initial gauge length and multiplying to 100, the Percent Creep Strain can be found. The tensile creep curve is obtained by plotting the percent creep strain against time. With an appropriate tensile-test machine, the extension and time can be accurately measured and plotted Figure 3.5. (Shah, 1984)

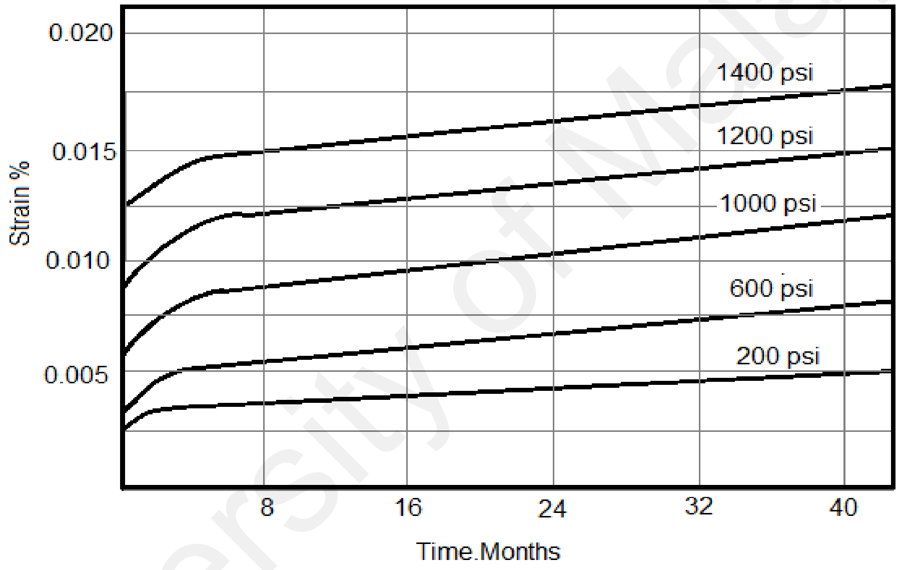

Figure 3.5 tensile creep curve at different loads

The main idea of flexure creep is to apply a constant load on the midspan of a flexure specimen which is slab shape, and measuring the deflection at specified time intervals, and the flexure creep curve is the creep strain against time. The Percent Flexure Creep Strain is calculated by $D\frac{rL^{2}}{6D}$(ASTM.D790, 2001) Where:

D = Maximum midspan deflection, mm (in.),
r = strain, mm/mm (in./in.),
d = depth of beam, mm (in.).
L = span, mm (in.), and

The maximum fiber stress can be calculated as follow if needed: $\sigma = \frac{3PL}{2bd^2}$

σ = stress in the outer fibers at midpoint, MPa (psi),
P = load at a given point on the load-deflection curve, N (lbf),
L = support span, mm (in.),
b = width of beam tested, mm (in.), and
d = depth of beam tested, mm (in.).

On this work, the focus is just on Tensile Creep Test.

3.3.3.2 Experimental procedure

As explained before there are one set of NBR and one set of CR samples, each has been divided into five batches which the first batch is dry, the second, third, fourth and fifth batch each immersed for one, two, three, and four weeks respectively (table 3.2) and then dried. Instron universal test machine was used to conduct the creep tensile test, but because of excessive swelling especially in CR rubbers after 2 weeks immersion some of the dumbbell's head needed to be cut in order to fit in the grips.

For starting the test the following items need to be set:

- The cross-section area of the middle part of the dumbbell A_0 after immersion which is used by the program to calculate the stress.

- The initial length L_i which is the distance between inner sides of the grips, it is also used by the machine to calculate the both true and engineering stress. (The true and engineering strain have been calculated separately as well)

- The strain rate which is set to 0.5 mm/s

- The force at which the creep is tested. For NBR the forces were chosen at 250N, 500N and 1000 Newton. And for CR the forces are at 200N, 400N and 600 Newton. The forces for CR have been selected less than NBR as CR shows weaker tensile test strength.

- The time in which the machine stops. This duration starts from the point the force reaches to the set value. On this work the time has been set to 1800 seconds (half an hour). There are two test specimens which underwent the test for 1200 second and on the diagrams can be recognized by the sudden discontinuity (the fractured specimens mostly show a sudden deviation).

By starting the test, the rubber is extended at a fixed strain rate (0.5 mm/s) till it gets under the defined force F, this period varies from specimen to specimen but once the load reached F the machine holds the force for 1800 seconds and record the length at every short interval.

The outputs of the Instron program at each interval are: Extension mm, Load N, Tensile stress MPa, Tensile extension mm, tensile strain%, true strain % and true stress.

3.3.3.3 Definitions of Terms Specific to This work:

The applied load is designated with F and the extension which is the increase in length from the start of the test to any specific time is shown by L_t. Point (*f*) has been defined as where the load reached to the set load for the first time Figure 3.6 and the time designated with t_f. By subtracting t_f from t, a new series of time would be created in which the test force start at time zero.

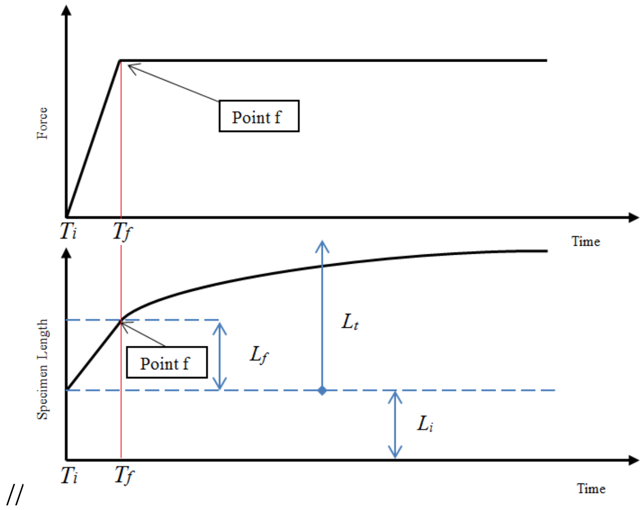

Figure 3.6 (Force –Time) & (Extention – Time) Diagrams

Other parameters are calculated based on the parameter of Figure 3.6 as follow:

Engineering strain:

$$\epsilon_{eng} = \frac{L_t - L_i}{L_i} \times 100 \tag{3.2}$$

Engineering creep strain: Just the data after point f are calculated

$$\epsilon_{eng-cr} = \frac{L_t - (L_f + L_i)}{L_f + L_i} \times 100 \tag{3.3}$$

True strain:

$$\epsilon_t = \ln \frac{L_i + L_t}{L_i} \tag{3.4}$$

True creep strain: Just the data after point f are calculated

$$\epsilon_{t-cr} = \ln \frac{L_i + L_t}{L_f + L_i} \tag{3.5}$$

Engineering stress:

$$\sigma = \frac{F}{A_0} \tag{3.6}$$

The engineering stress rises up to the point f and remains constant as A_0 and F are constant.

Creep modulus: It is one of the common ways to compare material creep behavior and is obtained by a simple dividing of initial applied stress by the True strain at any time. Plastics have a wide spectrum of retardation times, and elastic portions of strain cannot be separated in practice from nonelastic. Therefore, true strain is going to be used which refers to the sum of elastic strain plus the additional strain with time (ASTM.D2990, 2001).

$$E_{creep} \ @ \ time \ t = \frac{\sigma_0}{\epsilon_t @ \ time \ t} \tag{3.7}$$

Creep Modulus results from true creep strain: This is the how creep modulus is calculated in this work for generating the diagram. The formula offered by ASTM doesn't indicate accurate results.

$$E_{True \ creep \ strain} \ @ \ time \ t = \frac{\sigma_0}{\epsilon_{t-cr} @ \ time \ t} \tag{3.8}$$

Strain Rate: Strain rate or creep strain rate on this work defined as the slope of the *true strain versus time* diagram. Therefore, the instantaneous strain rate is

$$\dot{\epsilon} = \frac{\Delta\epsilon_t}{\Delta t} \tag{3.9}$$

Creep Rate: From the point (f) onward, the strain rate is called creep rate. Creep rate is one of the important parameters as in a condition like jet engine material is the stress needed to produce a creep rate of for example 1 % E/10 000 h. Figure 3.7

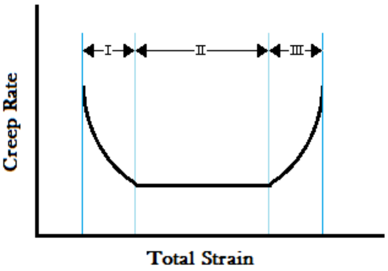

Figure 3.7 Creep rate – creep strain diagram (ASTM D2990)

3.3.3.4 Generating the diagrams

1- True Strain – Time: These diagrams are plotted true strain over time.

2- True Creep Strain – Time: These diagrams are plotted true creep strain over time.

3- Normalized True Strain – Time: After generating the true creep strain-time diagram for each specimen all the strains of a specimen are divided to the strain at point f (which is same as the initial strain), hence the first data would become the base with the value 1. By normalizing all the diagrams, the creep responses of different materials with different swelling level can be better compared. These diagrams are plotted the normalized true strain versus time.

4- Normalized Engineering Strain – Time: These diagrams are plotted the normalized engineering strain versus time. The purpose of having these diagrams is to compare the engineering with the true strain.

5- Creep Modulus – Time: These diagrams are generated by plotting Creep modulus versus time using logarithmic coordinates

6- Creep Rate – Normalized True Strain: these diagrams show the changes of creep rate over the changes of creep.

7- Creep rate – Time: these diagrams show the changes of creep rate over time.

CHAPTER 4 RESULTS AND DISCUSSION

4.1 Design of the device and the specimen

By looking closer to the overall design of the specimen and device Figure 4.1 and the experimental difficulties, the main advantages and disadvantages are summarized as below:

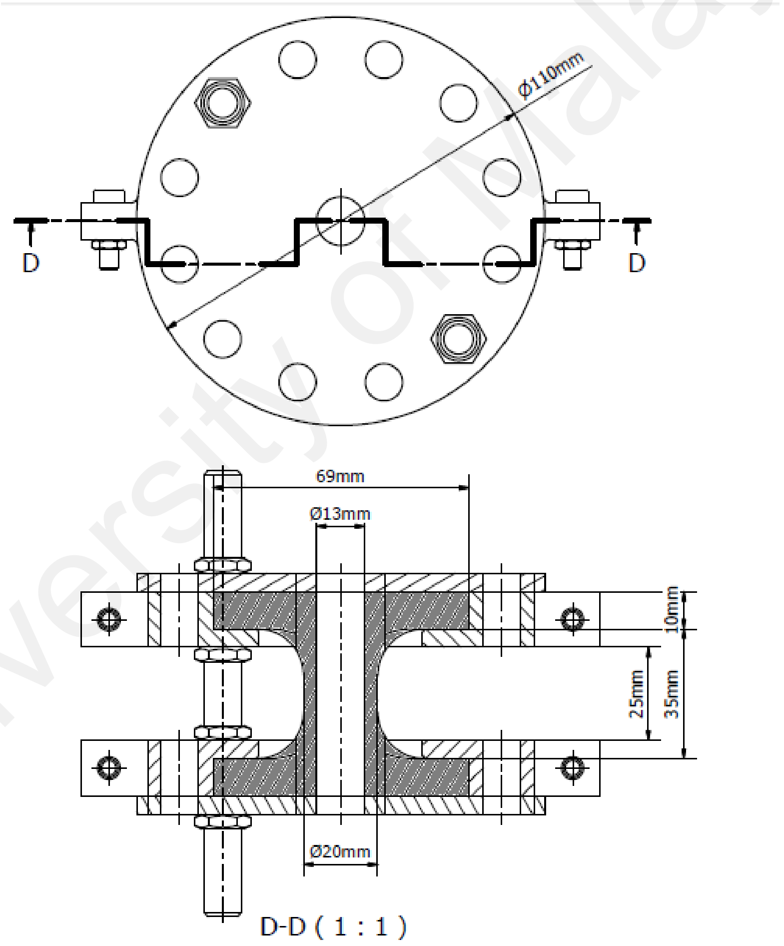

Figure 4.1 The cross section of the assembled specimen and grips

4.1.1 Advantages:

1. Multiaxial strain (stretching and twisting) can be introduced simultaneously to the specimens during the immersion test. This will allow the observation on the effect of mechanical loading on the diffusion of liquids.

2. Diffusion of liquids practically occurs only along radial direction, as the grips prevent oil diffusion covers the inner side of the head of the specimen and i.e. simple one dimension diffusion. Thus, the corresponding experimental results can be used to validate simple mechanical models for investigating the swelling of deformed elastomers.

3. Hollow diabolo specimen ensures that the equilibrium swelling can be achieved within a reasonable period of time while permitting the application of moderate compressive strain without buckling or wrinkling.

4. Different twist angles and axial extensions can be imposed to the specimen simply by fixing and adjusting bolts and nuts at appropriate positions.

5. No adhesive is used in the connection between the metallic part and the rubber specimen. Thus, immersion tests can be conducted using any types of aggressive liquids since debonding between rubber and metallic parts is not an issue.

6. The metallic grips and plates can be easily attached and dismantled from the rubber specimen.

7. The metallic grips are designed so that the device and specimen can be used for several subsequent mechanical testing, e.g. uniaxial tensile, simple torsion, combined torsion-tension or fatigue testing,which follow the immersion tests.

4.1.2 Disadvantages:

Although the device enables the experiment set up to be carried out successfully, there are some limitations that need to be investigated in future works:

1. Under simple torsion, the specimen is subjected to non-uniform strain (or stress) field. Being preliminary work, this additional difficulty dealing with diffusion of liquids in the presence of non-uniform strain (or stress) should be avoided. One possible way to obtain a relatively uniform strain and stress fields in the specimen under torsion would be by increasing its inner diameter while fixing its wall thickness.

2. Different parts in the specimen undergo different swelling levels due to its geometry and different exposure to the liquids. It is preferable to confine the diffusion, i.e. swelling, in the middle part of the specimen since this is the focus area of our study. This can be obtained by introducing appropriate sealing on the specimen such that diffusion takes place only through the inner and outer surfaces of the middle part of the specimen.

Once the swelling localizes at the middle part, the amount of swelling can be calculated by considering the change in volume or mass of the middle part only, and not the whole specimen, in order to obtain a precise value of swelling level under given mechanical loading. Works are currently in progress in order to overcome the above mentioned limitations and difficulties.

4.2 The effect of mechanical loading on swelling

Figure 4.2 shows the percentage of mass change of NBR immersed during one week in palm biodiesel under different loading conditions: stress-free S0T0, simple tension S20T0, simple torsion S0T30, S0T60, S0T90 and combined tension-torsion S20T30, S20T60, S20T90. For each condition, four specimens were tested. In the absence of tensile strain, the percentage of mass change varies from 1.4% to 1.9%. Meanwhile, in the presence of tensile strain, the percentage of mass change ranges from 2.1% to 2.6%. The effect of mechanical loading, in particularly tensile strain, on the amount of swelling is clearly shown in this figure. It is observed that the application of 20% tensile strain to the rubber specimen increases the amount of liquid uptake by as much as 50% regardless the amount of applied twist. In contrast, the effect of twist on the swelling level appears to be not as significant as the effect of tensile strain. Indeed, the application of twist increases only slightly the amount of liquid uptakes.

Similar immersion tests are conducted on CR specimens and the corresponding results are presented in Figure 4.3.It is found that for a given mechanical loading, the swelling level in CR is consistently higher than the one in NBR. The percentage of mass change in CR ranges from 4.5% to 6.0% in the absence of tensile strain and from 7.0% to 7.8% in the presence of tensile strain. Similarly to NBR, the tensile strain appears to have more significant effect than torsion on swelling level.

According to(Pekcan and Uğur, 2002), the high level of swelling in CR after immersion in palm biodiesel can be explained from molecular consideration: CR is made from emulsion polymerization of 2-chloro-1, 3-butadiene. Since the swelling of rubber is by the principle of “like dissolve like”, i.e. polar solvent are more likely to dissolve polar substances and non-polar substances are more likely to dissolve in non-polar solvent, the high polarity of ester in palm biodiesel favors the forming of polymer-solvent interaction in CR resulting to the increase of swelling in CR. The significant increase of swelling due to the application of tensile strain can be explained by the fact that the initial available surface of the specimen through which diffusion occurs increases. Moreover, tensile strain generates tensile stress in the material. In this case, the hydrostatic part of the stress is negative. According to Treloar (Treloar, 2005), negative hydrostatic part of the stress facilitates the liquid uptake resulting to higher swelling.(Ch’ng et al., 2013)

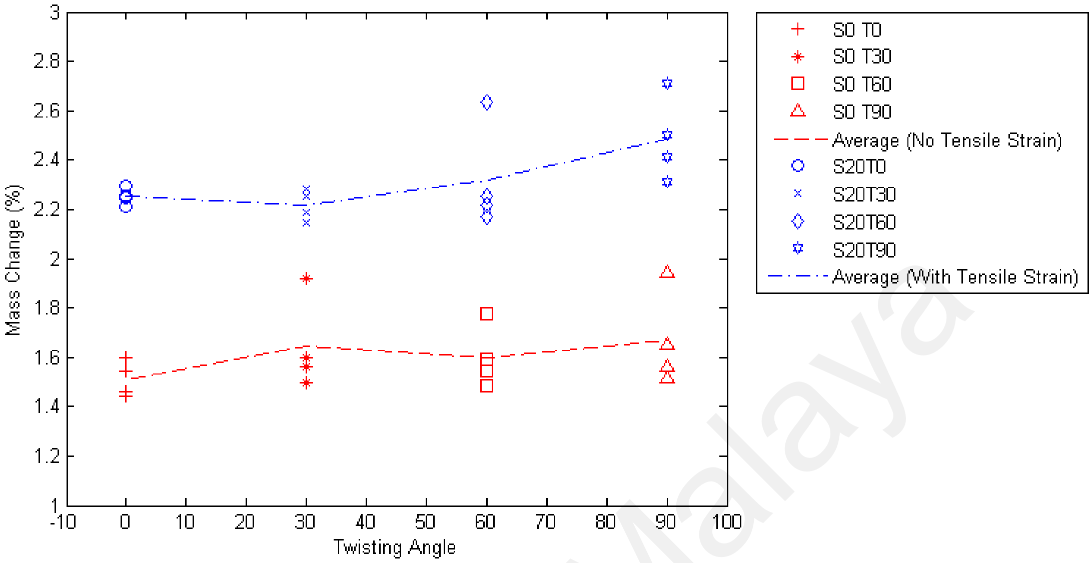

Figure 4.2 Mass change of NBR after 1 week immersion in palm biodiesel.(Ch’ng et al., 2013)

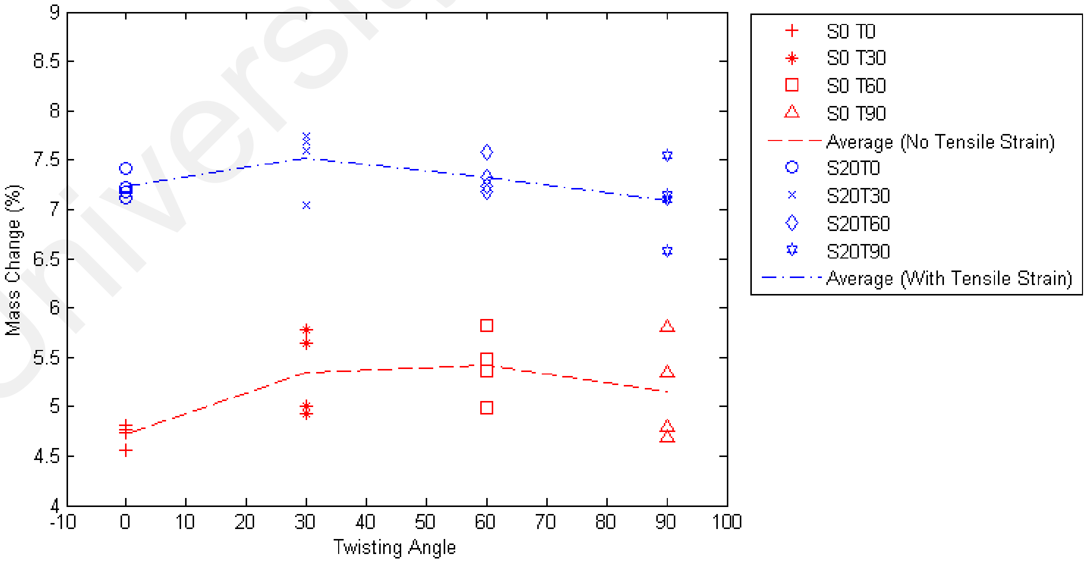

Figure 4.3 Mass change of CR after 1 week immersion in palm biodiesel(Ch’ng et al., 2013)

4.3 Creep test result

4.3.1 Swelling

All the tested specimens with their immersion duration and the percentage mass changes have been collected in Table 4.1, Based on the previous cyclic tests' data in the previous section the mass changes in the entire specimen increases by time due to the oil penetration. Figure 4.4 shows that the swelling in CR is significantly higher than NBR, as in the fourth week the mass change percentage of CR is 37.4% which is 5 times higher than that of NBR with 7.5%. This difference was discussed in the previous section (4.2).

Table 4.1 Mass Change Percentage of the specimens

Material	%weight gain after immersion		Material	%weight gain after immersion
NBR-dry-Tensile	-		**CR-dry-Tensile**	-
NBR-dry-250 N	-		**CR-dry-200 N**	-
NBR-dry-500 N	-		**CR-dry-400 N**	-
NBR-dry-1000 N	-		**CR-dry-600 N**	-
NBR-1 week-Tensile	3.420753843		**CR-1 week-Tensile**	15.19986158
NBR-1 week-250 N	3.476481309		**CR-1 week-200 N**	15.28303688
NBR-1 week-500 N	3.513306988		**CR-1 week-400 N**	15.30237471
NBR-1 week-1000 N	3.536875699		**CR-1 week-600 N**	14.78285125
NBR-2 week-Tensile	5.227212042		**CR-2 weeks-Tensile**	23.41110869
NBR-2 week-250 N	5.212252465		**CR-2 weeks-200 N**	21.66671955
NBR-2 week-500 N	5.229454686		**CR-2 weeks-400 N**	21.69300375
NBR-2 week-1000 N	5.282644248		**CR-2 weeks-600 N**	23.70231884
NBR-2 week-Tensile	6.443963312		**CR-3 weeks-Tensile**	30.97134985
NBR-2 week-250 N	6.319777512		**CR-3 weeks-200 N**	31.09677849
NBR-2 week-500 N	6.399529136		**CR-3 weeks-400 N**	31.30453957
NBR-2 week-1000 N	6.452376762		**CR-3 weeks-600 N**	31.38113337
NBR-2 week-Tensile	7.487148251		**CR-4 weeks-Tensile**	37.23819678
NBR-2 week-250 N	7.457185346		**CR4-weeks-200 N**	37.20433001
NBR-2 week-500 N	7.653680525		**CR-4 weeks-400 N**	37.60341011
NBR-2 week-1000 N	7.478113929		**CR4-weeks-600 N**	37.30311714

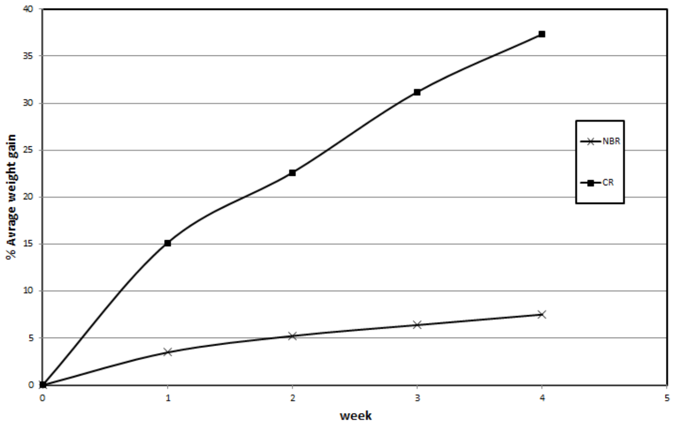

Figure 4.4 The mass change percentage (amount of swelling) during time

4.3.2 True Strain-Time

One of these diagrams (CR tested at 200 Newton) has been shown in Figure 4.5 and the rest in APPENDICES

Appendix 1: True Strain – Time Diagrams. On this diagram, it can be seen that the dry rubber elongated 14 percent up to the beginning of the test while the rubber, which immersed in oil for 4 weeks is elongated 25 percent, this shows that longer a rubber is left in the palm oil, softer they become and elongate more. These diagrams cannot predict the creep behaviors due to different initial stresses of the specimens. These diagrams cannot predict the creep behaviors due to different initial stresses of the

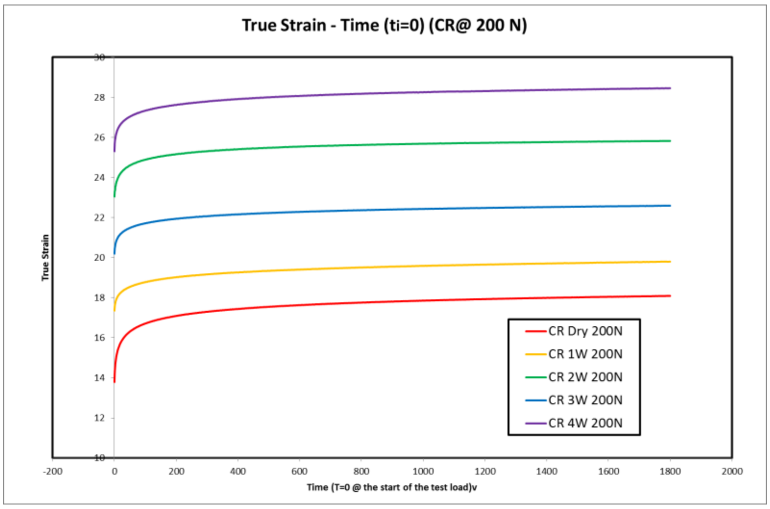

Figure 4.5 True Strain-Time (CR @ 200N)

specimens.

4.3.3 Normalized Creep Strain and Normalized Engineering Creep Strain

The Normalized Creep Strain gives the creep percentage to the initial strain. Here on Figure 4.6 the two series of diagrams has been shown, one by using the Normalized True Creep Strain data and the other one by using Normalized Engineering Creep Strain.

Normalized Creep Strain for CR   Normalized Engineering Strain for CR

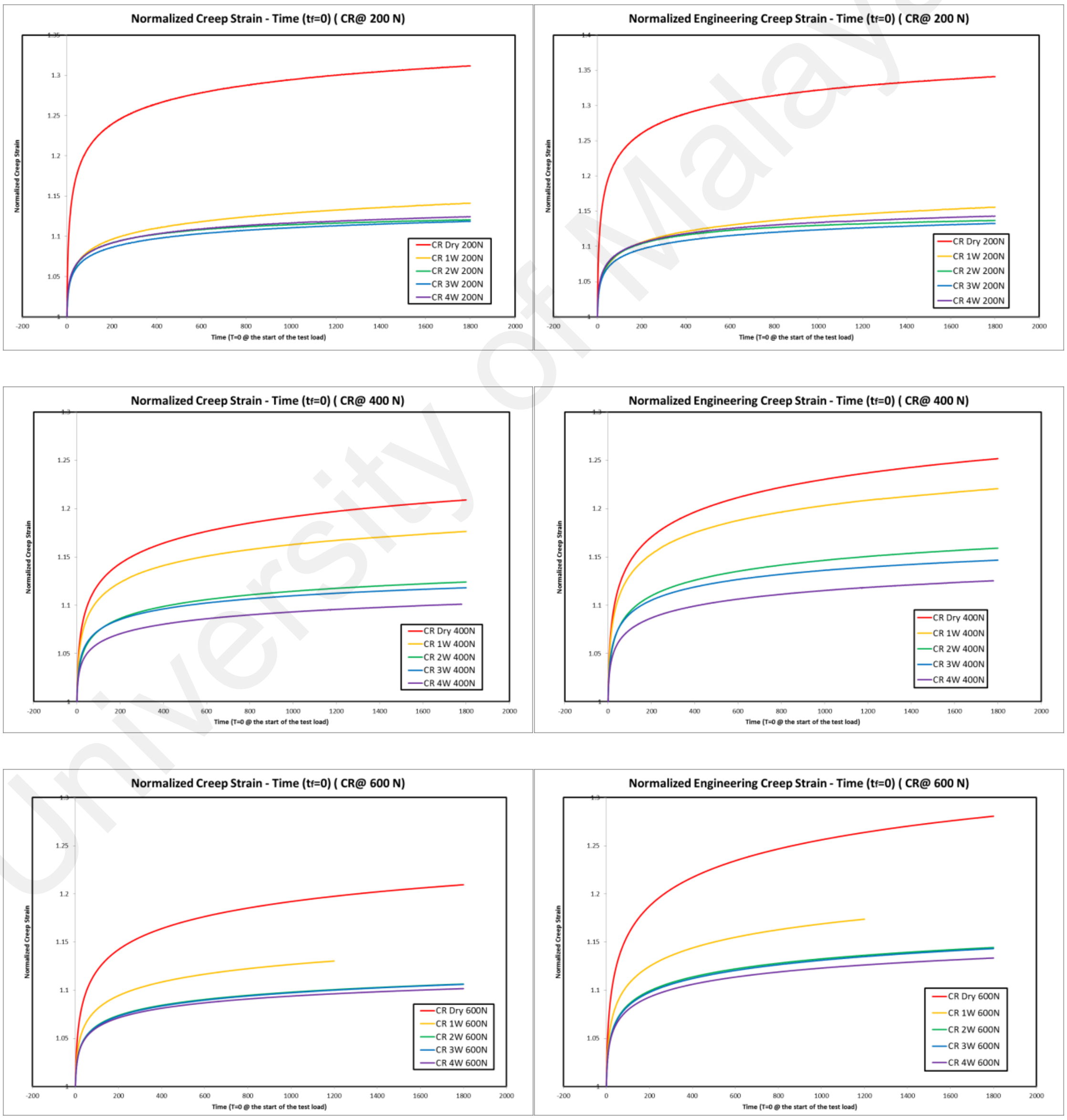

Figure 4.6 (Normalized Creep Strain) vs. (Normalized ENG Creep Strain)

The diagrams shows that there is not much variation between using the true strain formula and Engineering strain formula.

4.3.4 True Creep Strain – Time vs. Normalized Creep strain – Time

In True Creep Strain diagrams, the initial strains have been ignored and the curves depict the creeps after the set loads solely while Normalized Creep Strain diagrams show the creep percentage of the initial strain.

Figure 4.7 compares these diagrams for NBR Rubbers (for CR refer to Appendix 2: Creep Strain – Time Diagrams and Appendix 3: Normalized Creep Strain – Time Diagrams), in all the graphs the dry ones (red curves) are on top and show the highest creep strain over time followed by the one-week-immersed rubbers (yellow curves) which show the second highest creep. In addition, mostly the four-week-immersed rubbers (purple curves) show the least creep strain in both diagrams series. But not all the curves in both series follow the same trend as it can be seen, the two-week-immersed NBR rubber (green curve) has higher creep strain than three-week-immersed NBR rubber (blue curve) at 250 N in True Creep Strain Diagram while they are overlapped in Normalized Creep Strain. There is no significant difference in both diagrams at 500 N and at 1000N there are slight mismatches.

Considering Normalized Creep Strain a better approach over True Creep Strain due to having the influence of the initial strain, it can be observed that the creep is higher for unswollen rubbers and it decreases as the rubbers immersed more in the oil. These differences become less while the rubbers go under higher loads and immersed more in the oil. The last diagrams in Figure 4.7 shows that the curves of the two, three and four-week-immersed rubbers at 1000 N lie on each other. Same thing is true for CR rubbers (refer to Appendix 2: Creep Strain – Time Diagrams Appendix 3: Normalized Creep Strain – Time Diagrams).

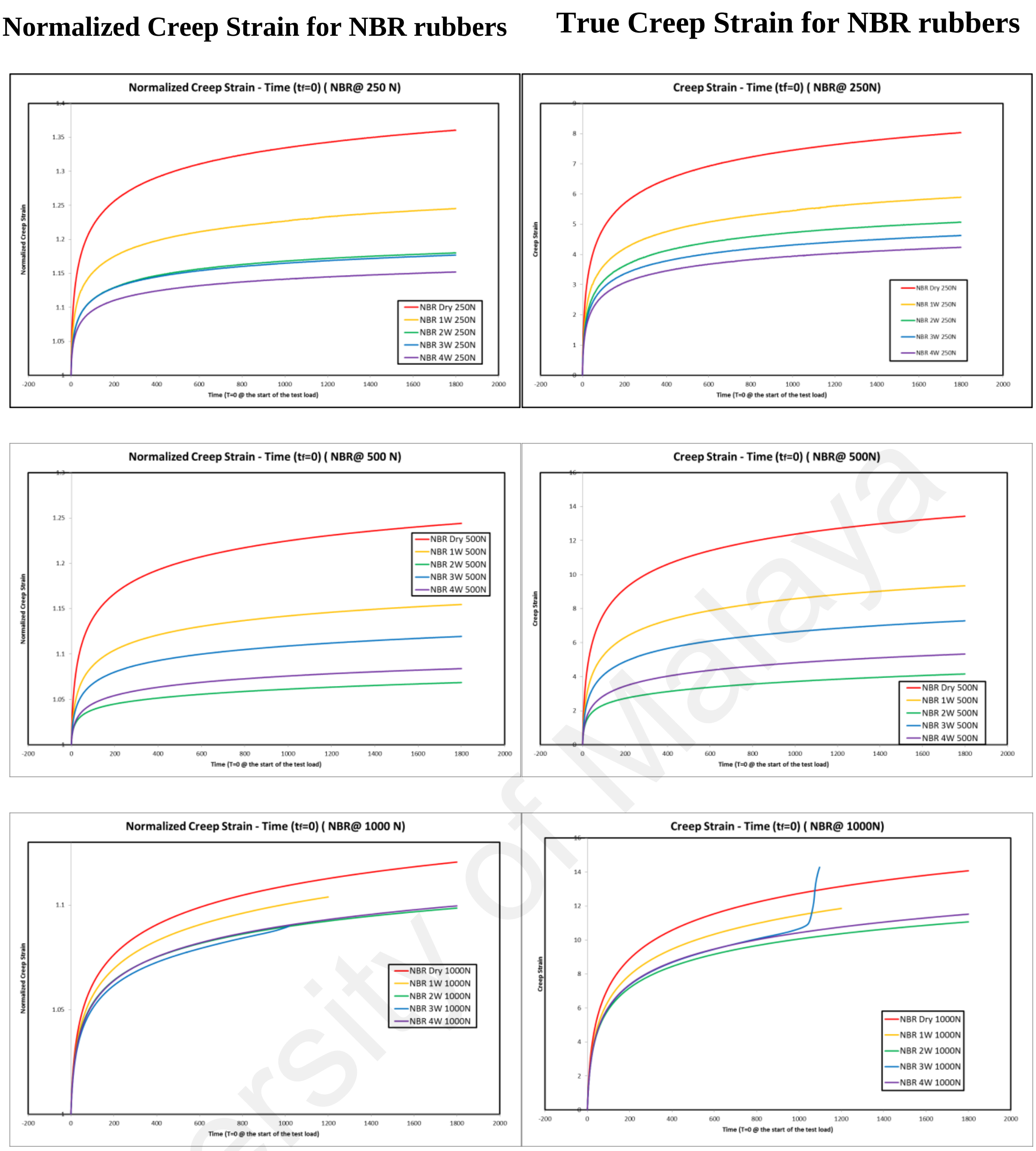

Figure 4.7 True Creep Strain – Time vs. Normalized Creep strain – Time

4.3.5 Creep Modulus – Time

Creep modulus is a factor for indicating material’s resistance to creep, higher the creep modulus is, more unlikely material should be to creep. The predictions from Normalized Creep strain – Time Diagrams, longer a rubber is immersed in the oil, less creep occurs. However, this is not the observation from creep modulus diagrams. Figure 4.8 shows the NBR’s Creep Modulus diagrams at left and CR’s at right and the only diagram that follows this trend is NBR at 500N. In three diagrams the creep modulus of the dry specimens are higher than the rest.

While the precise for having these fault is unclear, however one of the reasons could be due to the calculation of stress at any point by just the initial cross section area. During the initial strain the cross section area reduces significantly and this reduction is more noticeable for rubbers immersed longer as they are softer.

Creep Modulus Diagram of NBR

Creep Modulus Diagram of CR

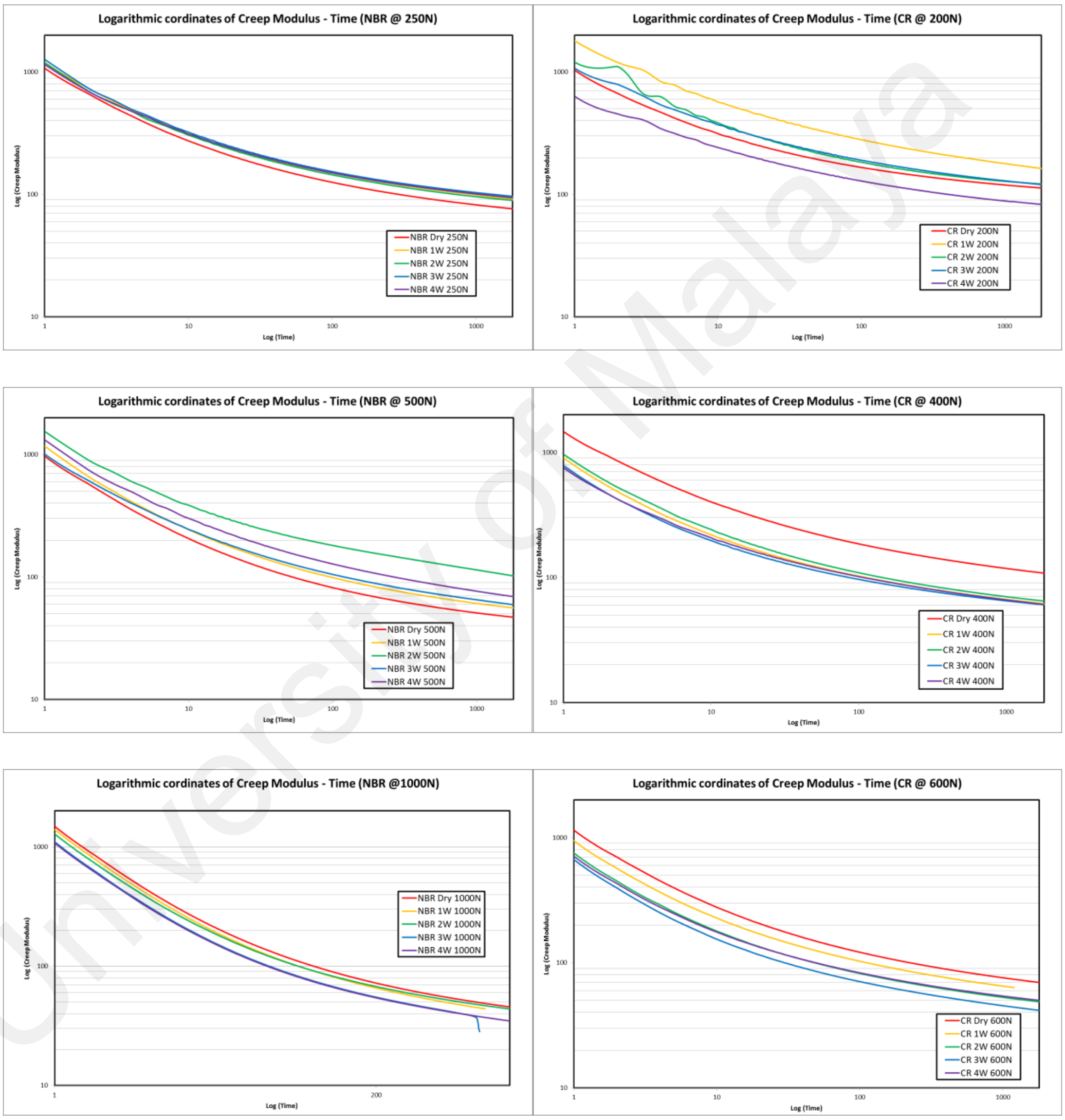

Figure 4.8 Creep Modulus-Time Diagrams

4.3.6 Creep Rate – Time and Creep Rate – Normalized True Strain

The Creep Rate – Time diagrams Appendix 5: Creep Strain Rate - Time show that the rate of creep at any point for drier rubbers are higher than the swollen ones and decrease by time. The Figure 4.9 Creep Strain Rate – Time shows this trend for CR rubbers creped at 200 Newton.

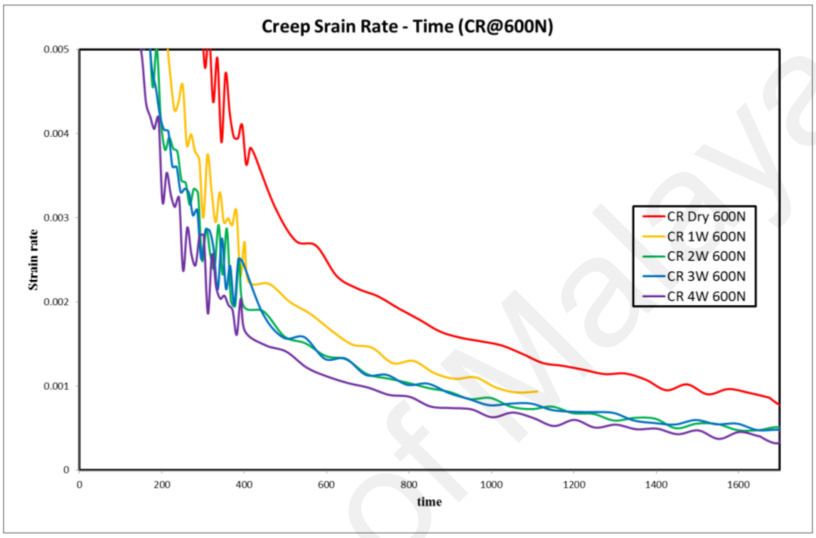

Figure 4.9 Creep Strain Rate – Time for CR at 600N

The Creep Rate over Normalized Creep diagrams explain the same trends, the creep rates are higher in drier rubbers and decreases while the creep progress. Figure 4.10 shows the Diagram For NBR at 250 Newton.

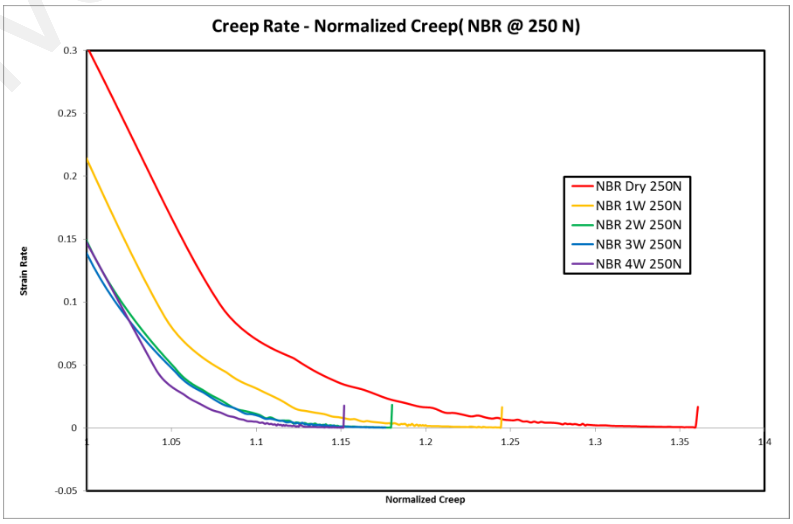

Figure 4.10 Creep Strain Rate – Normalized Creep for NBR at 250N

CHAPTER 5 CONCLUSIONS AND RECOMMENDATION

5.1 Conclusions

Novel experimental specimen and device for the investigation of swelling of rubber in the presence of multiaxial large strain has been developed. The device consists of a hollow diabolo rubber specimen attached to specially-designed circular metallic grips and plates such that immersion tests can be conducted while the specimens are simultaneously subjected to various mechanical loading conditions: simple tension, simple torsion and combined tension-torsion.

The levels of swelling experienced by both NBR and CR are found to be significantly affected by the presence of mechanical loading. More precisely, the effect of tensile strain appeared to be more significant than that of torsion. It was found that the swelling level increases significantly when a tensile strain is introduced. Moreover, slight increase in swelling is observed when a twist is applied. The increase of swelling due to the application of torsion is in contrast to the observation of Treloar. Our results suggest that the corresponding discrepancy could be attributed to the specimen geometry.

Creep occurs in rubbers when they elongate by time under constant load, this work confirms that the penetration of oil inside the intermolecular structure of rubbers, weaken the material by breaking the secondary bonding and results the material to become softer and less resistance to deformation. The creep rate of materials follow the same trends as softer materials have higher creep rate at the beginning of the test (initial strain) and show slower creep rate during the test.

It was observed that creep occurs in both dry and swollen rubbers; moreover, the creep was found to be more significant in dry one than in swollen one this is consistence with the previous work of (Chai et al., 2013) as the palm biodiesel appears to act as lubricant facilitating movement of the polymer chain segments.

5.2 Recommendation

Creep Modulus, which is one of the most common ways to investigate the creep behavior of materials, need to be reviewed. The formula for Creep Modulus offered by (ASTM.D2990, 2001) lacks of accuracy due to using the total strain as the initial strain as it varies for different materials. The Creep Modulus formula on this work (using Creep-Strain) seems more accurate but the cross section area need to be calculated at each point for more accurate results.

REFERENCES:

ASTM.D412 1998. Standard Test Methods for Vulcanized Rubber and Thermoplastic Elastomers—Tension.

ASTM.D790 2001. Standard Test Methods for Flexural Properties of Unreinforced and Reinforced Plastics and Electrical Insulating Materials.

ASTM.D2990 2001. Standard Test Methods for Tensile, Compressive, and Flexural Creep and Creep-Rupture of Plastics.

BOWER, A. F. 2010. *Applied Mechanics of Solids*, CRC PressINC.

CALLISTER, W. D. 2007. *Materials Science And Engineering: An Introduction*, John Wiley & Sons.

CH'NG, S. Y., ANDRIYANA, A., VERRON, E., KAHBASI, O. & AHMAD, R. 2013. Development of a Novel Experimental Device to Investigate Swelling of Elastomers in Biodiesel Undergoing Multiaxial Large Deformation. *Experimental Mechanics***,** 1-10.

CHAGNON, G., VERRON, E., MARCKMANN, G. & GORNET, L. 2006. Development of new constitutive equations for the Mullins effect in rubber using the network alteration theory. *International Journal of Solids and Structures,* 43**,** 6817-6831.

CHAI, A. B., ANDRIYANA, A., VERRON, E. & JOHAN, M. R. 2013. Mechanical characteristics of swollen elastomers under cyclic loading. *Materials & Design,* 44**,** 566-572.

COLUMBIA ENGINEERING RUBBER, I. 2012. Columbia Compound Information (http://www.columbiaerd.com/materials.html).

DE WITH, G. 2006. *Structure, Deformation, and Integrity of Materials: Plasticity, visco-elasticity, and fracture*, Wiley-VCH.

DELATYCKI, O. 1971. *Mechanical performance and design in polymers*, Interscience Publishers.

DEMIRBAS, A. 2009. Progress and recent trends in biodiesel fuels. *Energy Conversion and Management,* 50**,** 14-34.

DWIVEDI, G., JAIN, S. & SHARMA, M. P. 2011. Impact analysis of biodiesel on engine performance—A review. *Renewable and Sustainable Energy Reviews,* 15**,** 4633-4641.

FLORY, P. J. 1953. *Polymer Chemistry*, Cornell University Press.

FRIED, J. R. 2003. *Polymer Science and Technology*, Prentice Hall Professional Technical Reference.

FUKUMORI, K., KURAUCHI, T. & KAMIGAITO, O. 1990. Swelling behaviour of rubber vulcanizates: 2. Effects of tensile strain on swelling. *Polymer,* 31**,** 2361-2367.

GOVINDJEE, S. & SIMO, J. 1992. Transition from micro-mechanics to computationally efficient phenomenology: Carbon black filled rubbers incorporating mullins' effect. *Journal of the Mechanics and Physics of Solids,* 40**,** 213-233.

HASEEB, A. S. M. A., JUN, T. S., FAZAL, M. A. & MASJUKI, H. H. 2011. Degradation of physical properties of different elastomers upon exposure to palm biodiesel. *Energy,* 36**,** 1814-1819.

LIU, A. F. 2005. *Mechanics and Mechanisms of Fracture: An Introduction*, ASM International.

LIU, I. S. 2002. *Continuum Mechanics*, Springer.

LOKE, K. M., DICKINSON, M. & TRELOAR, L. R. G. 1972. Swelling of a rubber cylinder in torsion: Part 2. Experimental. *Polymer,* 13**,** 203-207.

MCCARTHY, P., RASUL, M. G. & MOAZZEM, S. 2011. Analysis and comparison of performance and emissions of an internal combustion engine fuelled with petroleum diesel and different bio-diesels. *Fuel,* 90**,** 2147-2157.

MULLINS, L. 1948. Effect of Stretching on the Properties of Rubber. *Rubber Chemistry and Technology,* 21**,** 281-300.

O'TOOLE 1968. *Creep Properties of Plastics*, McGraw Hill.

OGDEN, R. W. 1997. *Non Linear Elasic Deformations*, Dover Publ.

PEKCAN, Ö. & UĞUR, Ş. 2002. Molecular weight effect on polymer dissolution: a steady state fluorescence study. *Polymer,* 43**,** 1937-1941.

PETERS, A. & CANDAU, S. J. 1988. Kinetics of swelling of spherical and cylindrical gels. *Macromolecules,* 21**,** 2278-2282.

PRASERTSAN, S. & PRASERTSAN, P. 1996. Biomass residues from palm oil mills in Thailand: An overview on quantity and potential usage. *Biomass and Bioenergy,* 11**,** 387-395.

RAM, A. 1997. *Fundamentals of polymer engineering*, Plenum Press.

ROBERTS, A. J. 1994. *Continuum Mechanics*, World Scientific.

SEALS, S. 2012. Oring Technical Center (http://orings.com).

SHAH, V. 1984. *Handbook of plastics testing technology*, Wiley.

SRINATH, L. S. 2009. *Adv Mechanics Of Solids 3E*, McGraw-Hill Education (India) Pvt Limited.

STRONG, A. B. 2006. *Plastics: materials and processing*, Pearson Prentice Hall.

TAN, H. T., LEE, K. T. & MOHAMED, A. R. 2010. Second-generation bio-ethanol (SGB) from Malaysian palm empty fruit bunch: Energy and exergy analyses. *Bioresource Technology,* 101**,** 5719-5727.

TRAKARNPRUK, W. & PORNTANGJITLIKIT, S. 2008. Palm oil biodiesel synthesized with potassium loaded calcined hydrotalcite and effect of biodiesel blend on elastomer properties. *Renewable Energy,* 33**,** 1558-1563.

TRELOAR, L. R. G. 2005. *The physics of rubber elasticity*, Oxford, Oxford Univ. Press.

APPENDICES

Appendix 1: True Strain – Time Diagrams

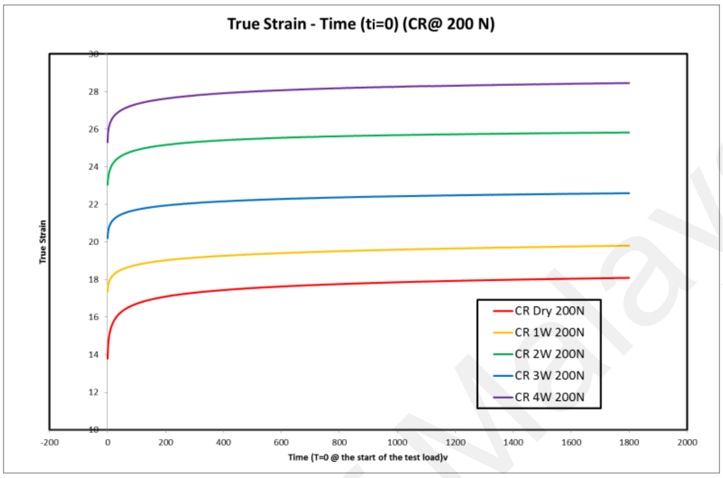

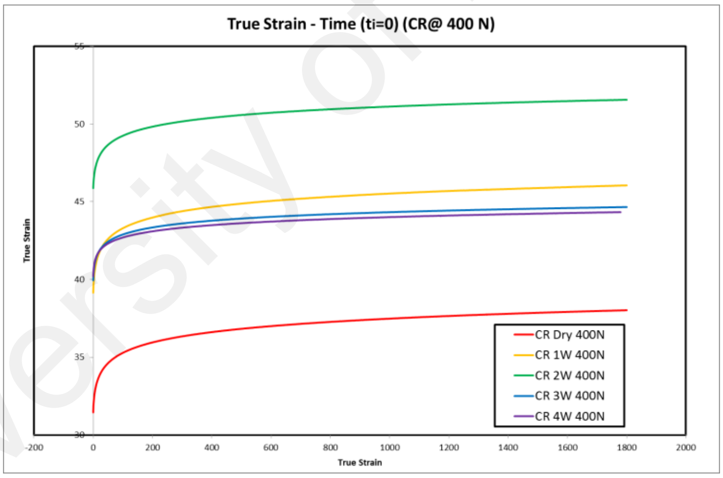

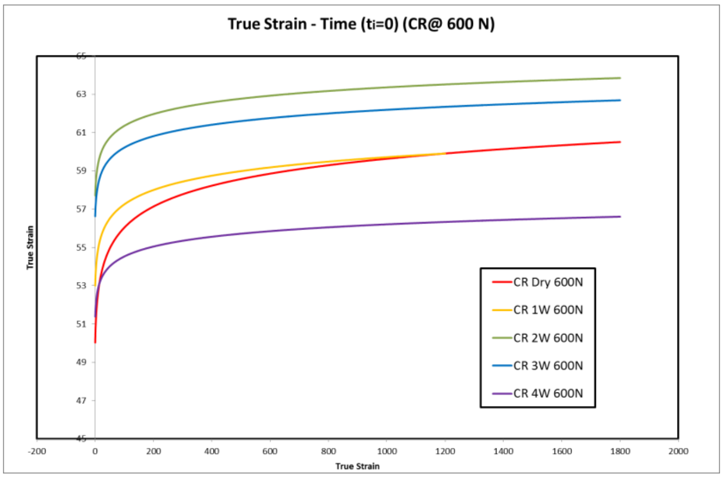

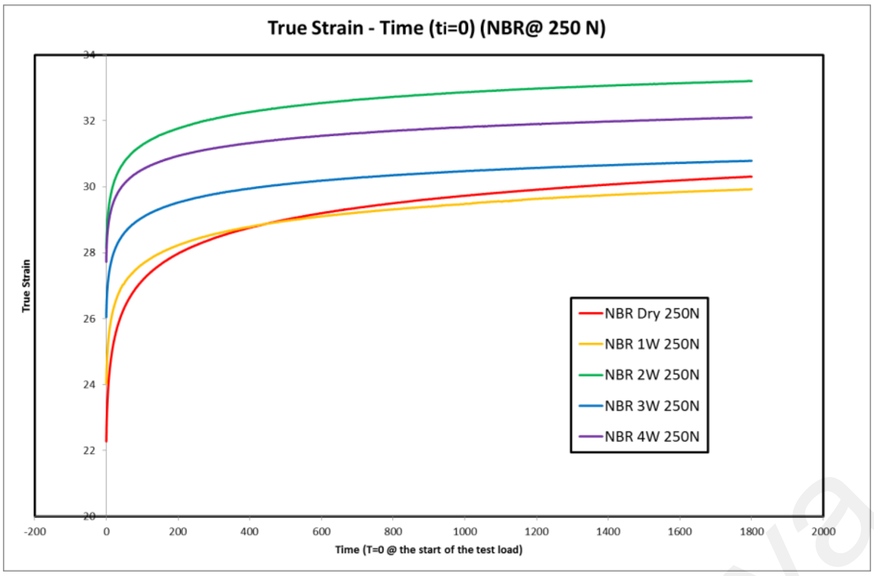
True Strain - Time (ti=0) (NBR@ 250 N)
True Strain
34
32
30
28
26
24
22
20
-200
0
200
400
600
800
1000
1200
1400
1600
1800
2000
Time (T=0 @ the start of the test load)
NBR Dry 250N
NBR 1W 250N
NBR 2W 250N
NBR 3W 250N
NBR 4W 250N

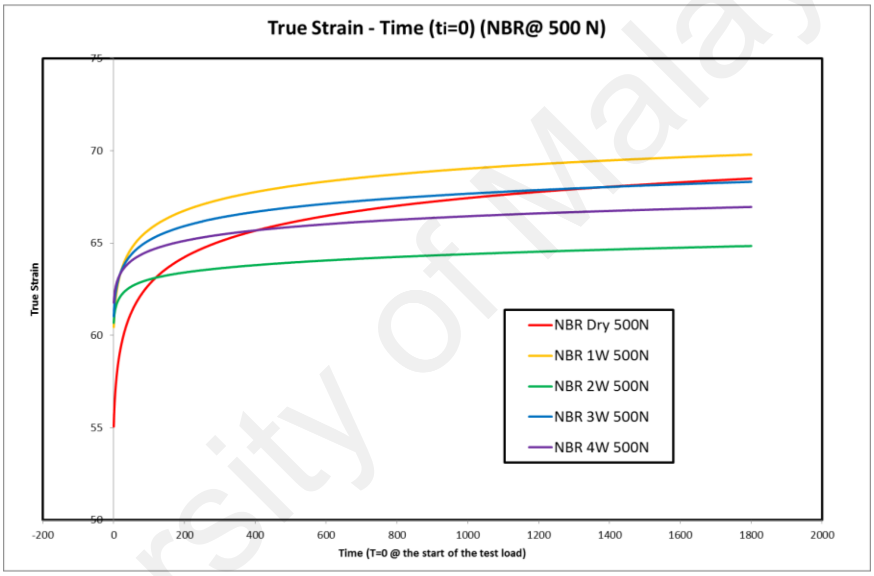
True Strain - Time (ti=0) (NBR@ 500 N)
True Strain
75
70
65
60
55
50
-200
0
200
400
600
800
1000
1200
1400
1600
1800
2000
Time (T=0 @ the start of the test load)
NBR Dry 500N
NBR 1W 500N
NBR 2W 500N
NBR 3W 500N
NBR 4W 500N

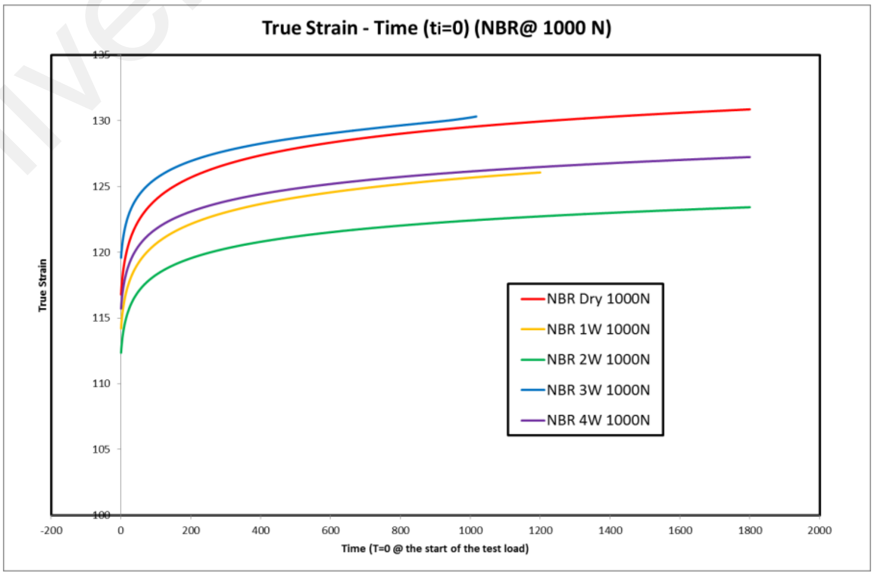
True Strain - Time (ti=0) (NBR@ 1000 N)
True Strain
135
130
125
120
115
110
105
100
-200
0
200
400
600
800
1000
1200
1400
1600
1800
2000
Time (T=0 @ the start of the test load)
NBR Dry 1000N
NBR 1W 1000N
NBR 2W 1000N
NBR 3W 1000N
NBR 4W 1000N

Appendix 2: Creep Strain – Time Diagrams

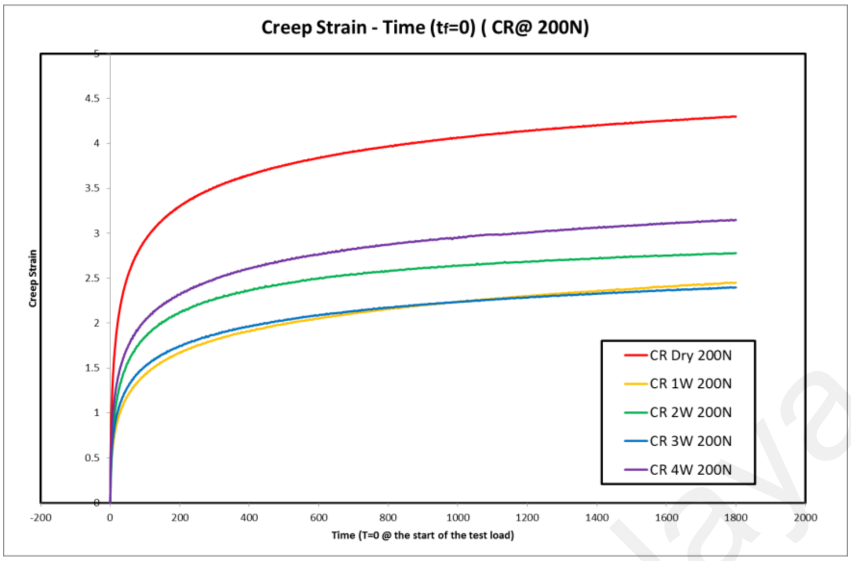

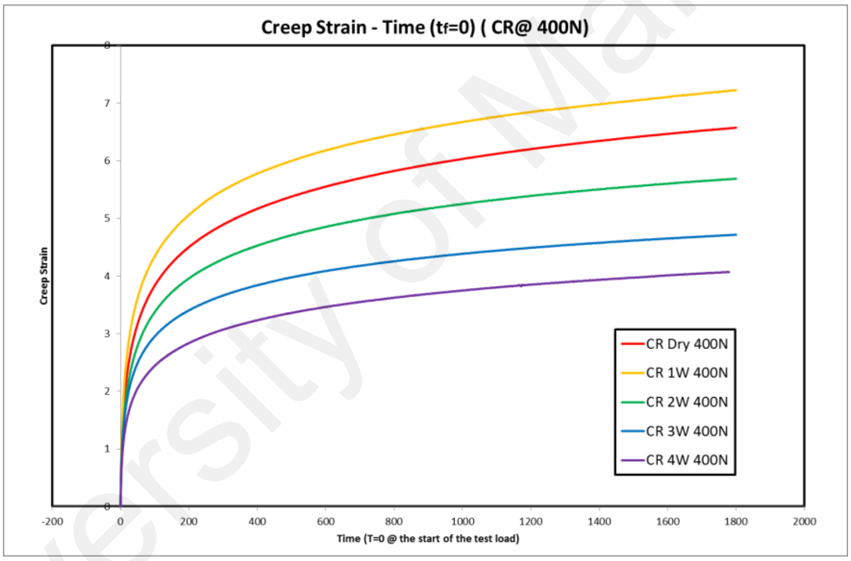

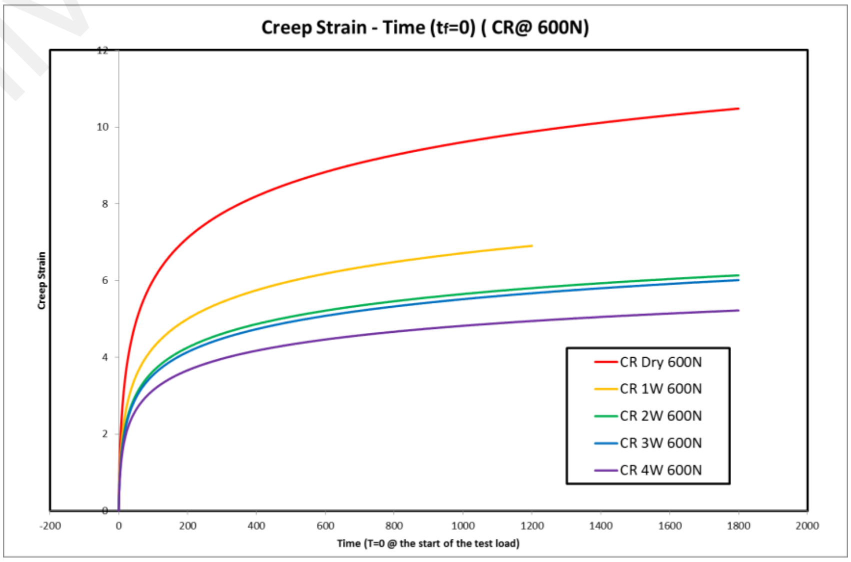

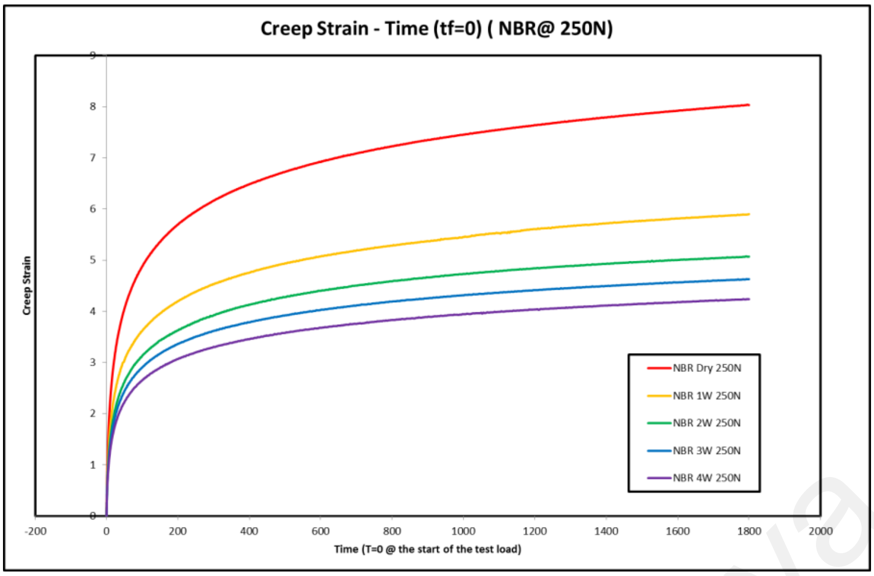
Creep Strain - Time (tf=0) (NBR@ 250N)
Creep Strain
0
1
2
3
4
5
6
7
8
9
-200
0
200
400
600
800
1000
1200
1400
1600
1800
2000
Time (T=0 @ the start of the test load)
NBR Dry 250N
NBR 1W 250N
NBR 2W 250N
NBR 3W 250N
NBR 4W 250N

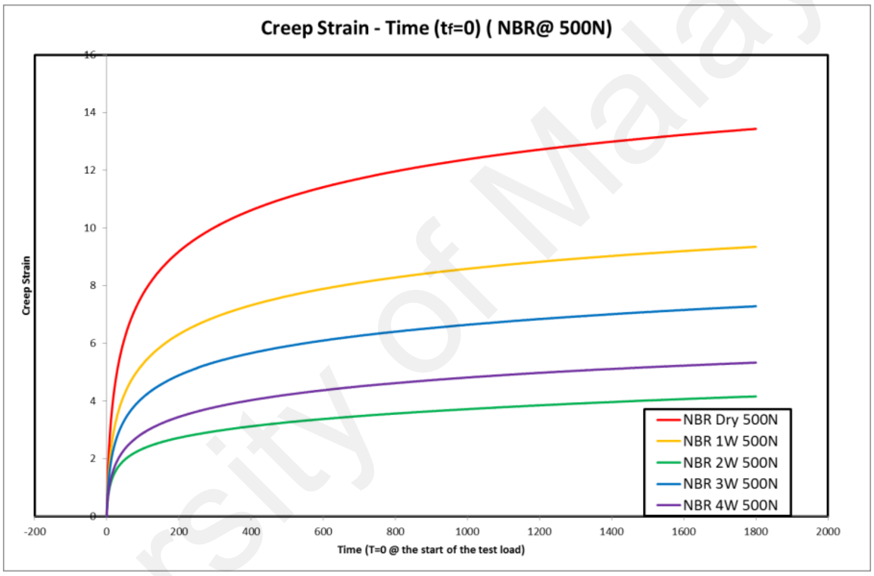
Creep Strain - Time (tf=0) (NBR@ 500N)
Creep Strain
0
2
4
6
8
10
12
14
16
-200
0
200
400
600
800
1000
1200
1400
1600
1800
2000
Time (T=0 @ the start of the test load)
NBR Dry 500N
NBR 1W 500N
NBR 2W 500N
NBR 3W 500N
NBR 4W 500N

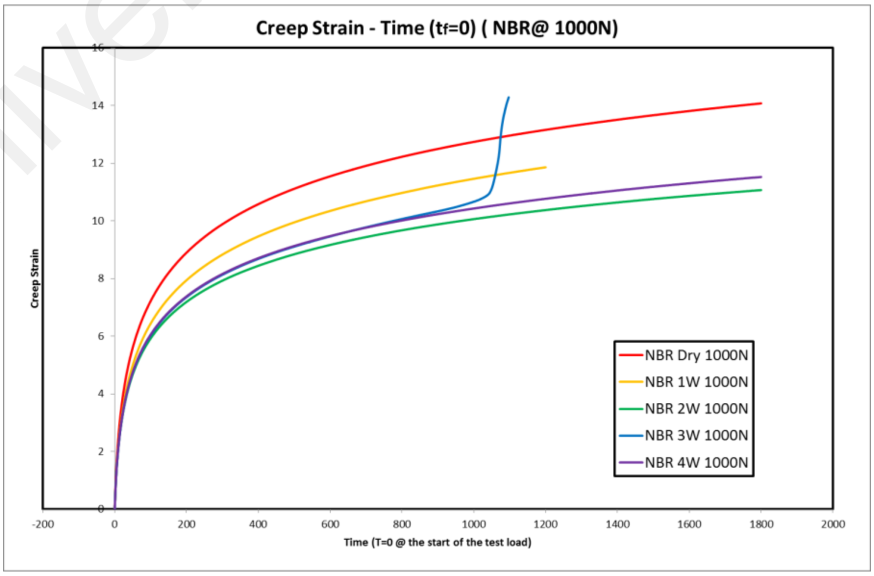
Creep Strain - Time (tf=0) (NBR@ 1000N)
Creep Strain
0
2
4
6
8
10
12
14
16
-200
0
200
400
600
800
1000
1200
1400
1600
1800
2000
Time (T=0 @ the start of the test load)
NBR Dry 1000N
NBR 1W 1000N
NBR 2W 1000N
NBR 3W 1000N
NBR 4W 1000N

Appendix 3: Normalized Creep Strain – Time Diagrams

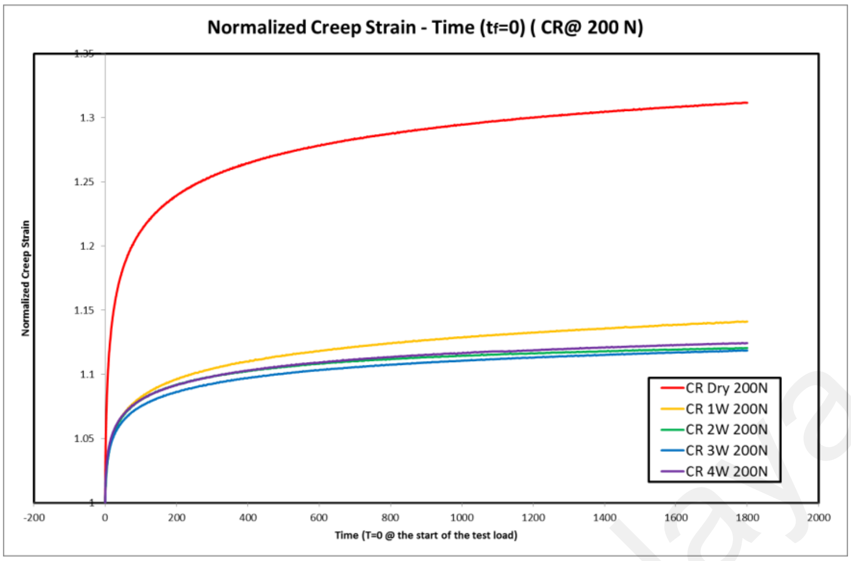

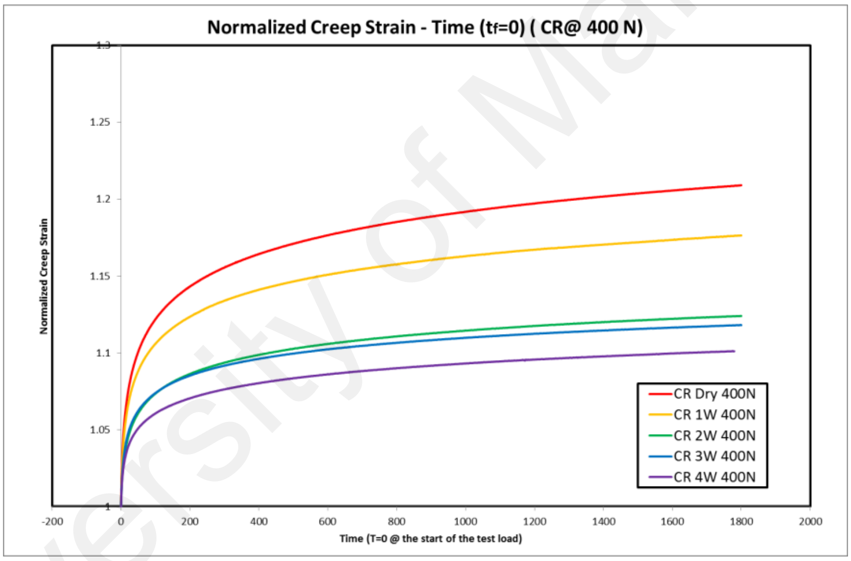

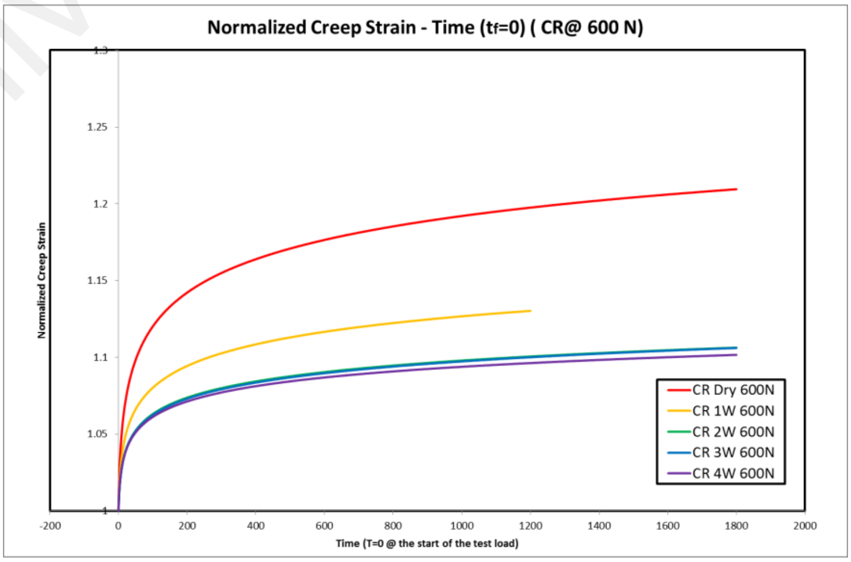

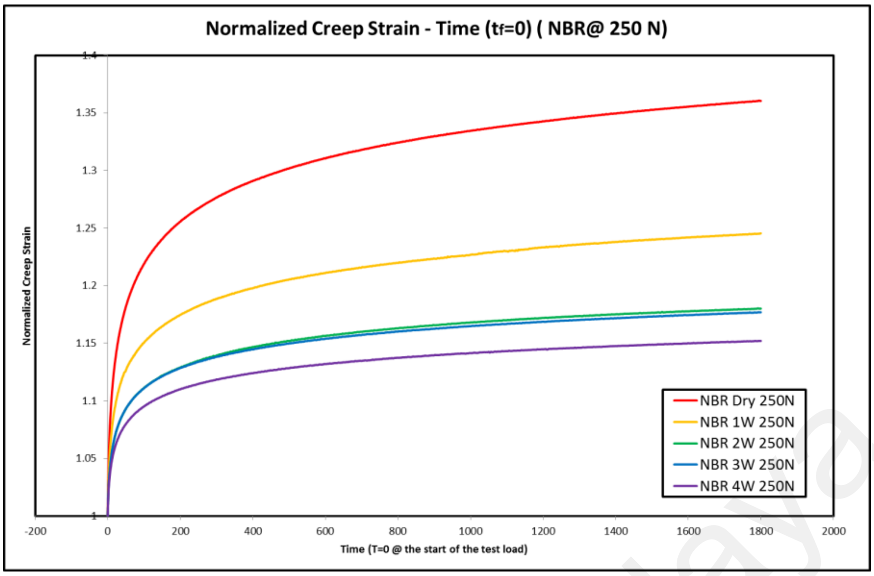
Normalized Creep Strain - Time (tf=0) (NBR@ 250 N)
Normalized Creep Strain
1.4
1.35
1.3
1.25
1.2
1.15
1.1
1.05
1
-200
0
200
400
600
800
1000
1200
1400
1600
1800
2000
Time (T=0 @ the start of the test load)
NBR Dry 250N
NBR 1W 250N
NBR 2W 250N
NBR 3W 250N
NBR 4W 250N

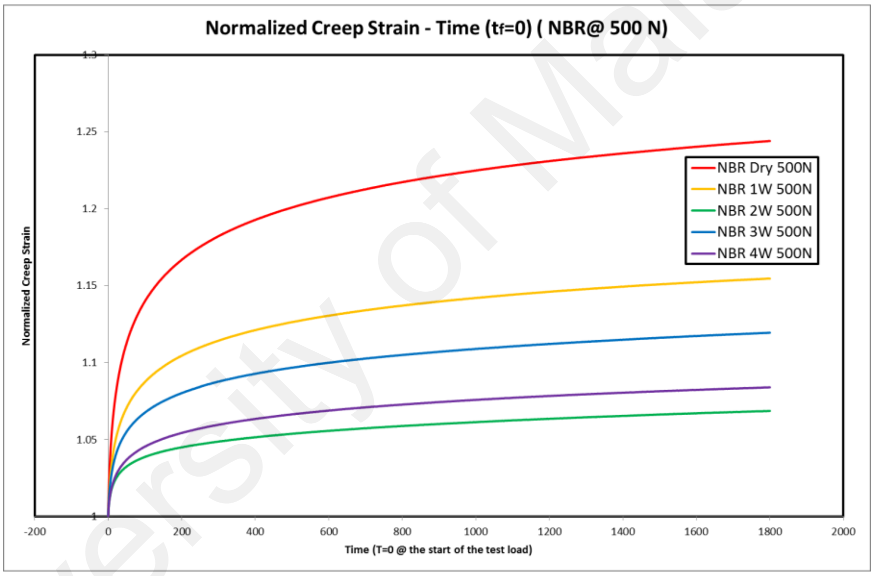
Normalized Creep Strain - Time (tf=0) (NBR@ 500 N)
Normalized Creep Strain
1.3
1.25
1.2
1.15
1.1
1.05
1
-200
0
200
400
600
800
1000
1200
1400
1600
1800
2000
Time (T=0 @ the start of the test load)
NBR Dry 500N
NBR 1W 500N
NBR 2W 500N
NBR 3W 500N
NBR 4W 500N

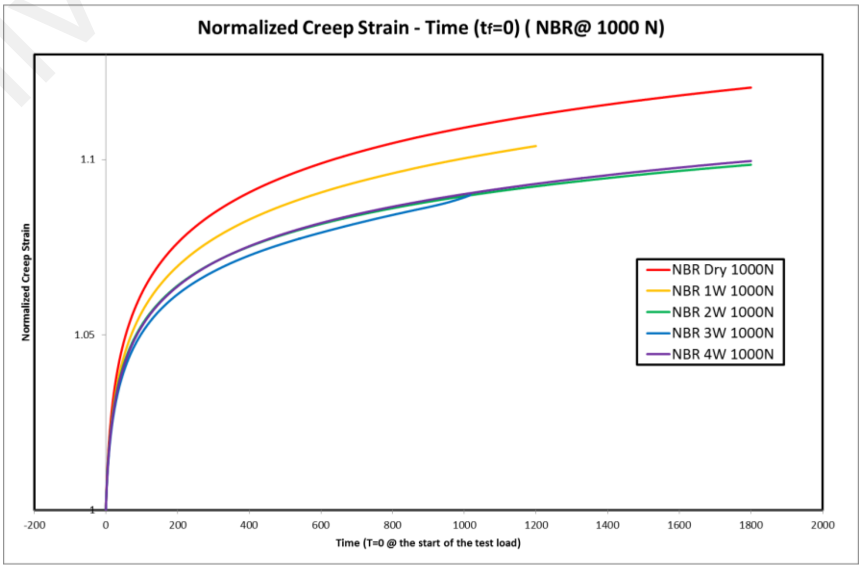
Normalized Creep Strain - Time (tf=0) (NBR@ 1000 N)
Normalized Creep Strain
1.1
1.05
1
-200
0
200
400
600
800
1000
1200
1400
1600
1800
2000
Time (T=0 @ the start of the test load)
NBR Dry 1000N
NBR 1W 1000N
NBR 2W 1000N
NBR 3W 1000N
NBR 4W 1000N

Appendix 4: (Normalized Creep Strain) vs (Normalized ENG Creep Strain)

Normalized Creep Strain for CR	Normalized Engineering Strain for CR

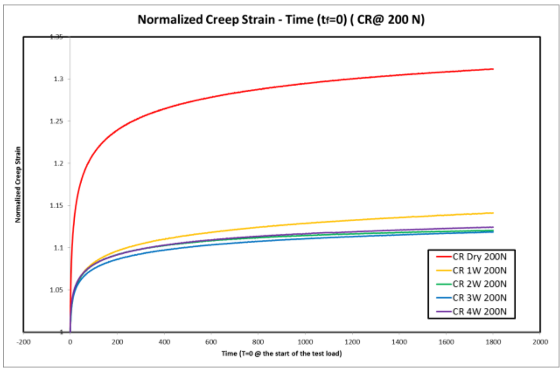

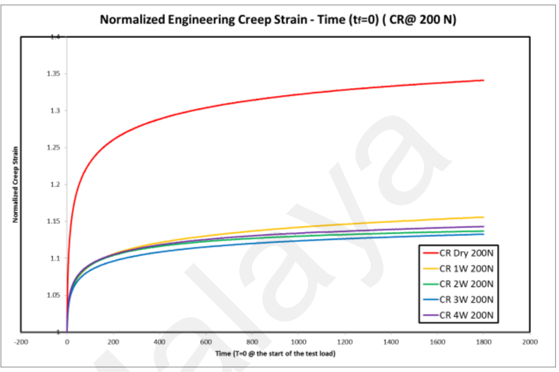

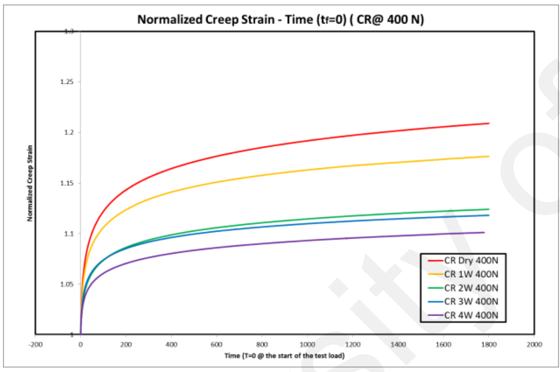

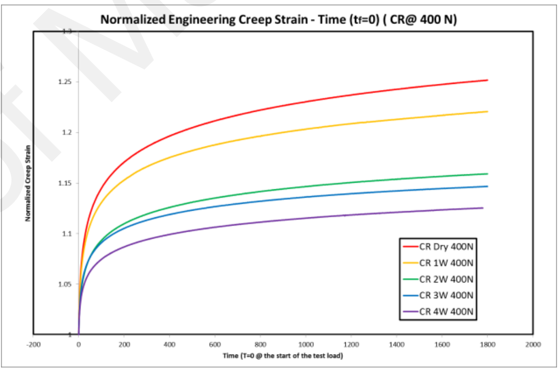

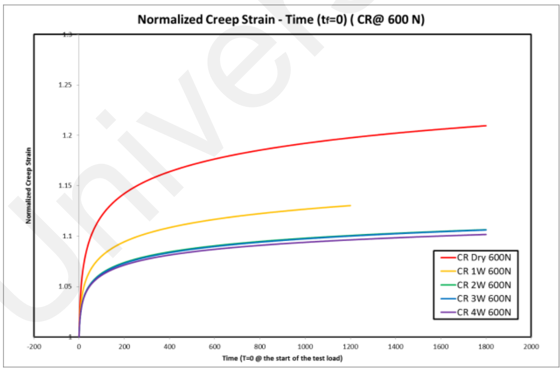

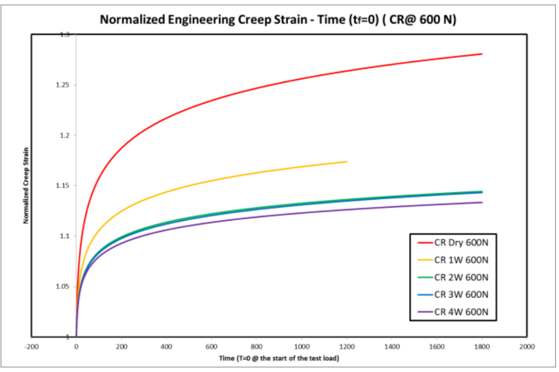

Normalized Creep Strain for NBR	Normalized Engineering Strain for NBR

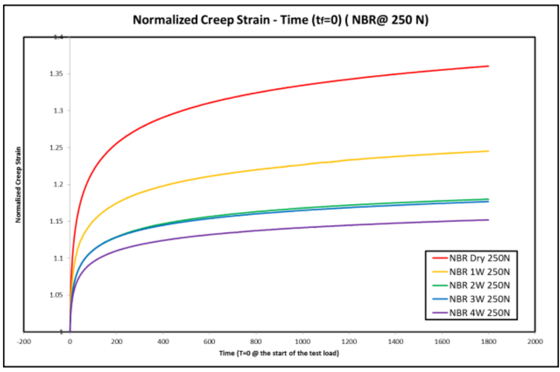

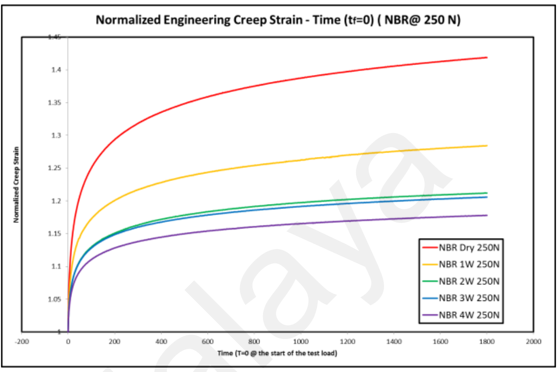

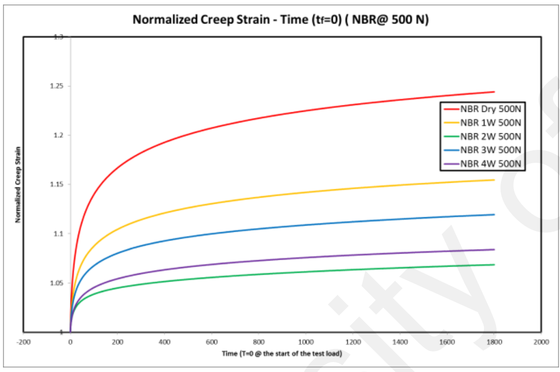

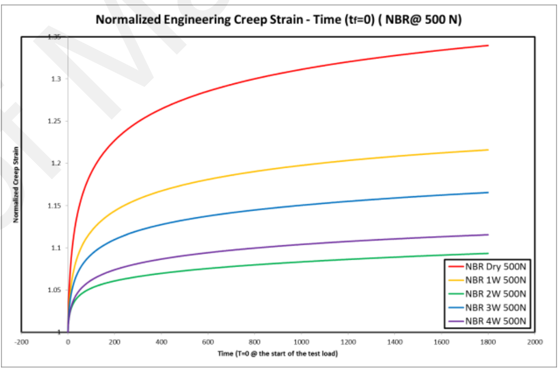

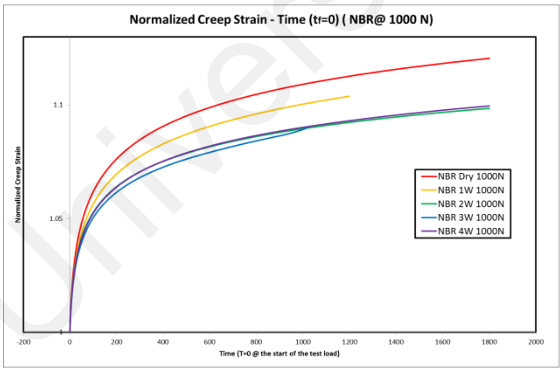

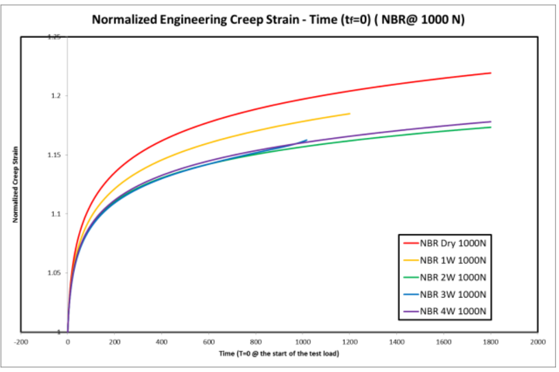

Appendix 5: Creep Modulus - Time

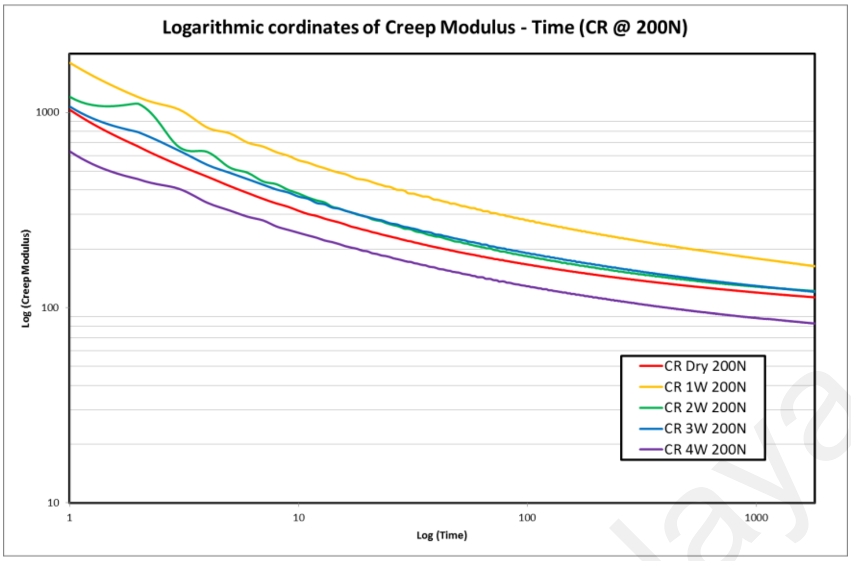

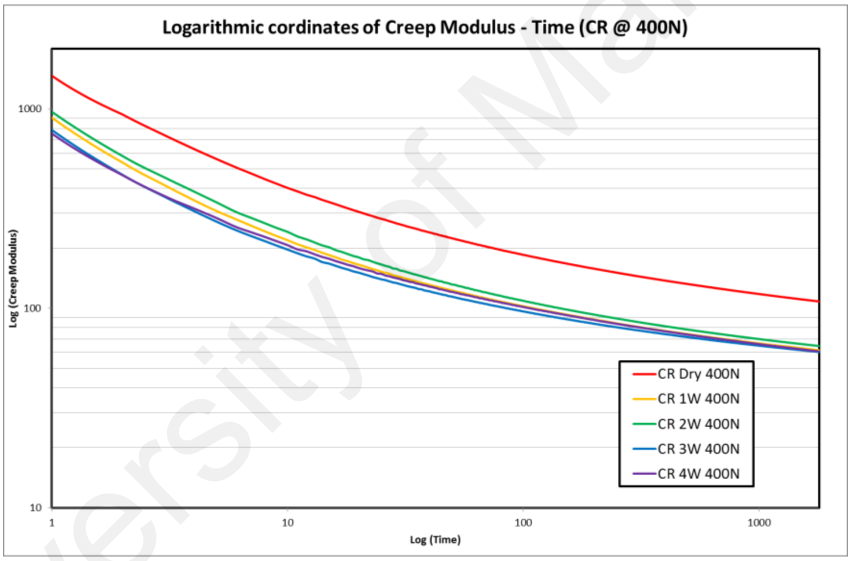

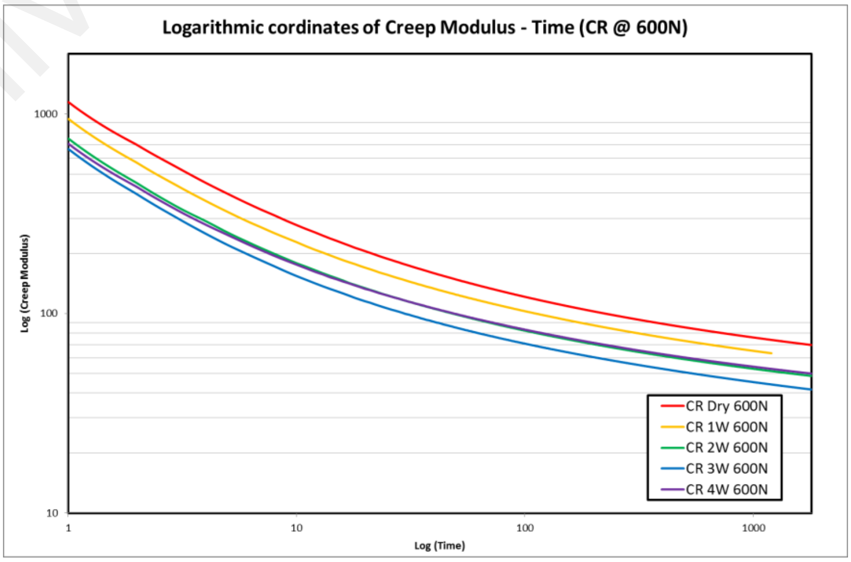

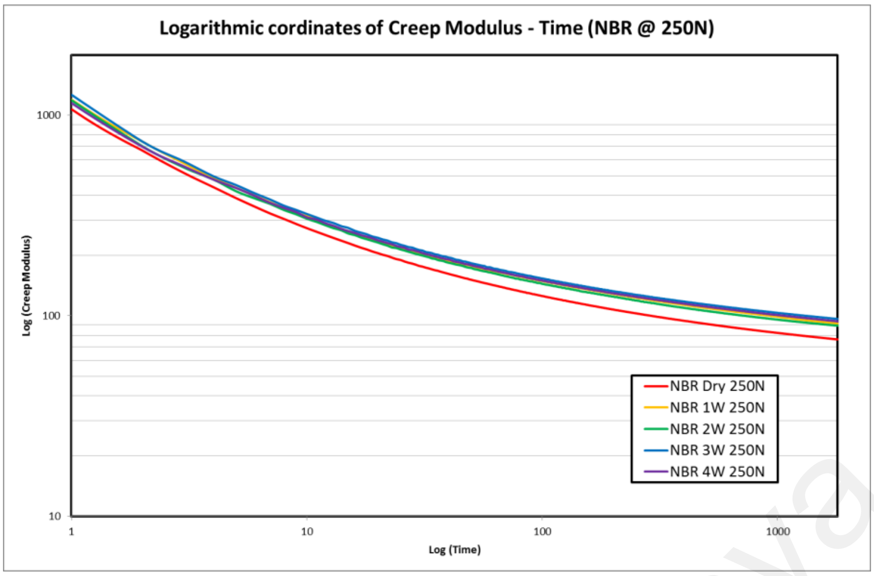
Logarithmic cordinates of Creep Modulus - Time (NBR @ 250N)
Log (Creep Modulus)
1000
100
10
1
10
100
1000
Log (Time)
NBR Dry 250N
NBR 1W 250N
NBR 2W 250N
NBR 3W 250N
NBR 4W 250N

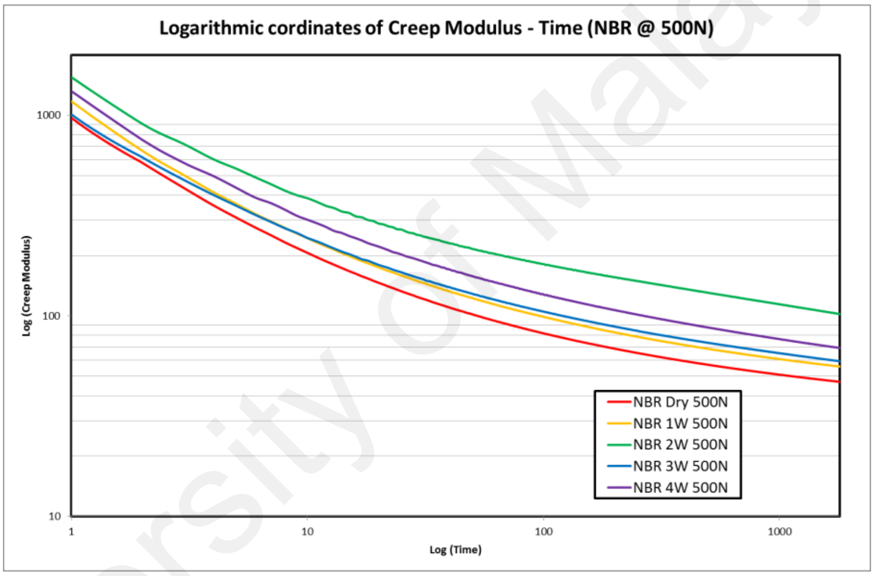
Logarithmic cordinates of Creep Modulus - Time (NBR @ 500N)
Log (Creep Modulus)
1000
100
10
1
10
100
1000
Log (Time)
NBR Dry 500N
NBR 1W 500N
NBR 2W 500N
NBR 3W 500N
NBR 4W 500N

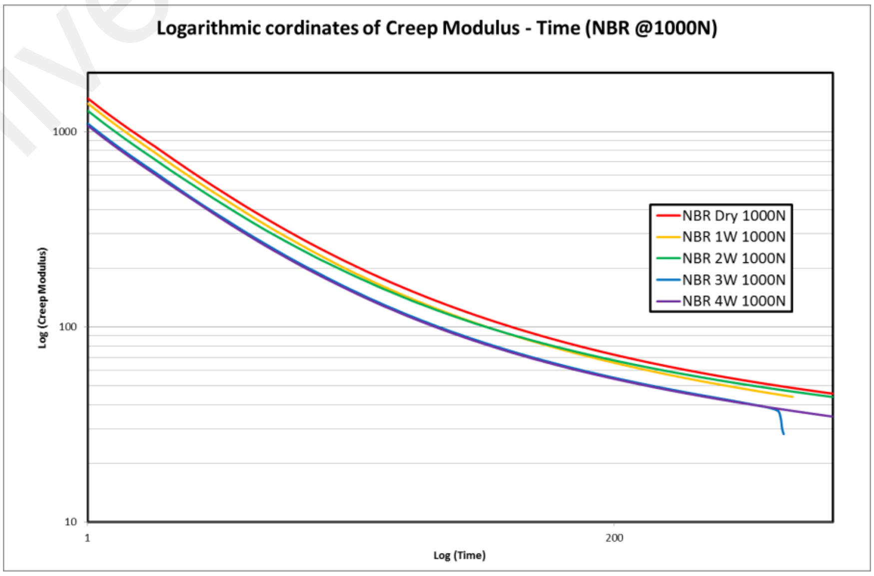
Logarithmic cordinates of Creep Modulus - Time (NBR @1000N)
Log (Creep Modulus)
1000
100
10
1
200
Log (Time)
NBR Dry 1000N
NBR 1W 1000N
NBR 2W 1000N
NBR 3W 1000N
NBR 4W 1000N

Appendix 5: Creep Strain Rate - Time

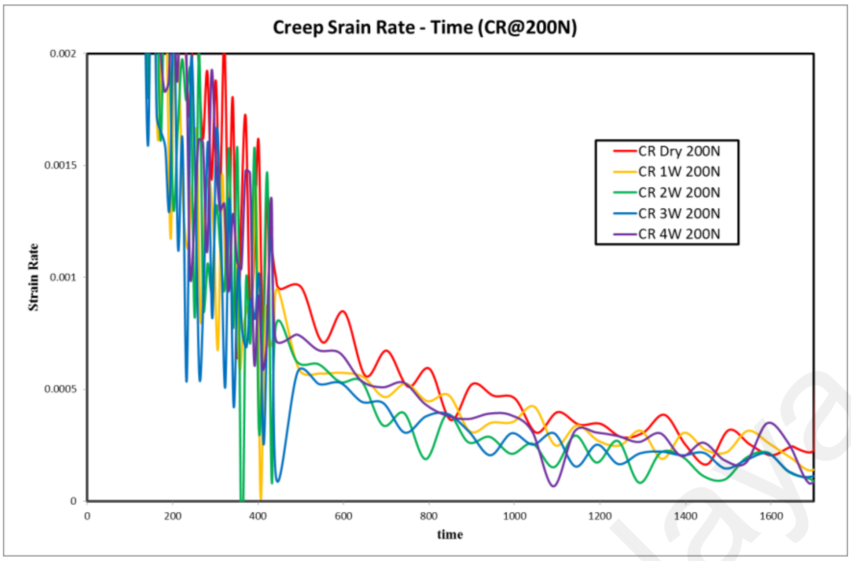

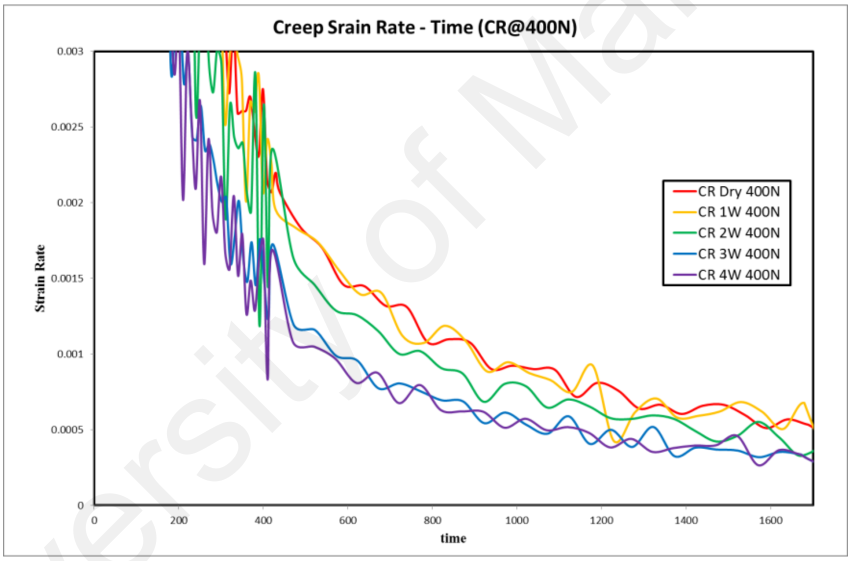

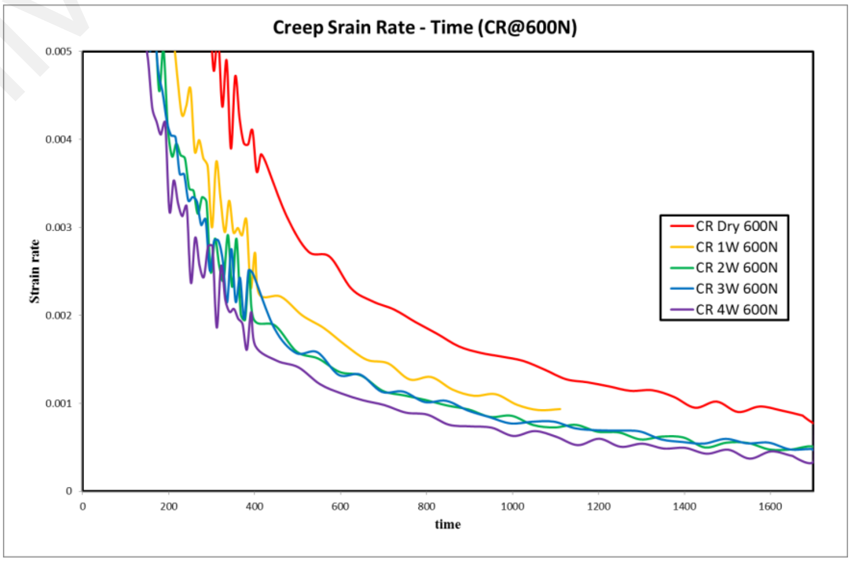

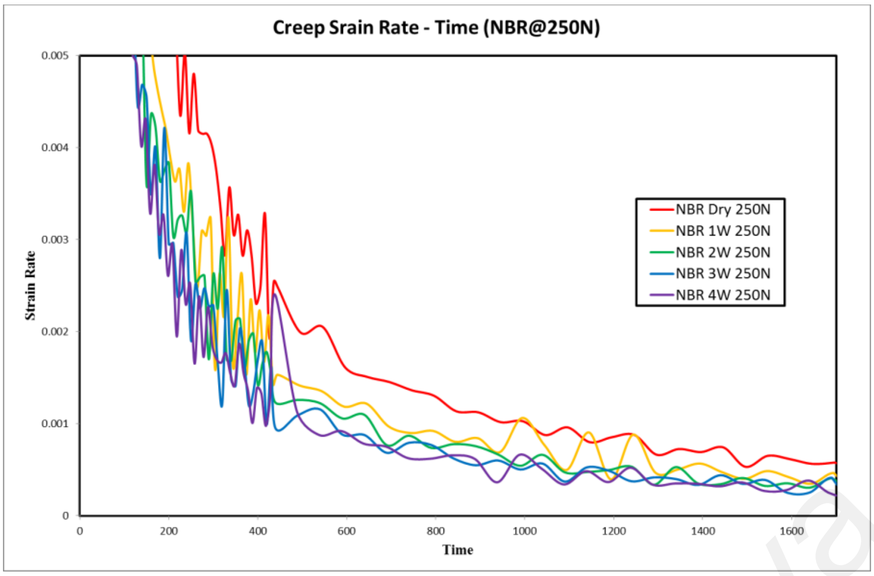
Creep Srain Rate - Time (NBR@250N)
Strain Rate
0.005
0.004
0.003
0.002
0.001
0
0
200
400
600
800
1000
1200
1400
1600
Time
NBR Dry 250N
NBR 1W 250N
NBR 2W 250N
NBR 3W 250N
NBR 4W 250N

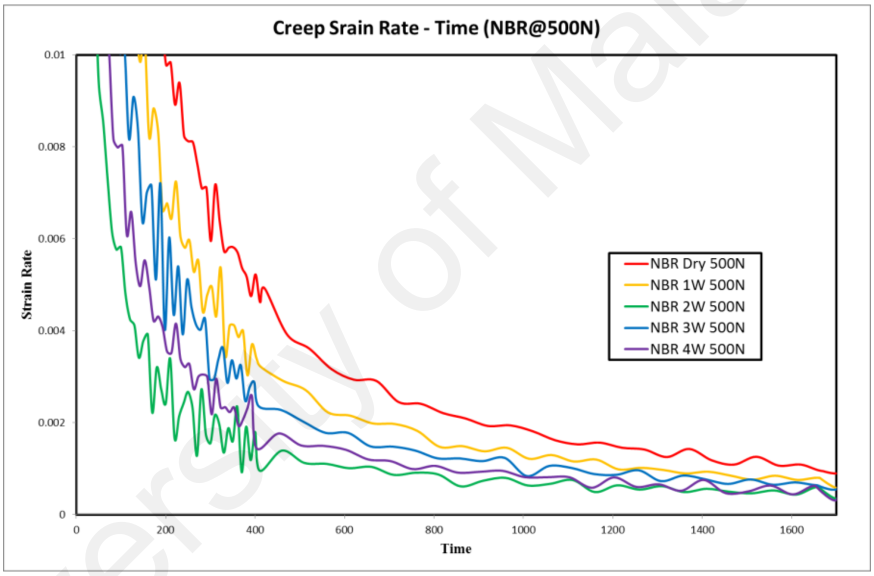
Creep Srain Rate - Time (NBR@500N)
Strain Rate
0.01
0.008
0.006
0.004
0.002
0
0
200
400
600
800
1000
1200
1400
1600
Time
NBR Dry 500N
NBR 1W 500N
NBR 2W 500N
NBR 3W 500N
NBR 4W 500N

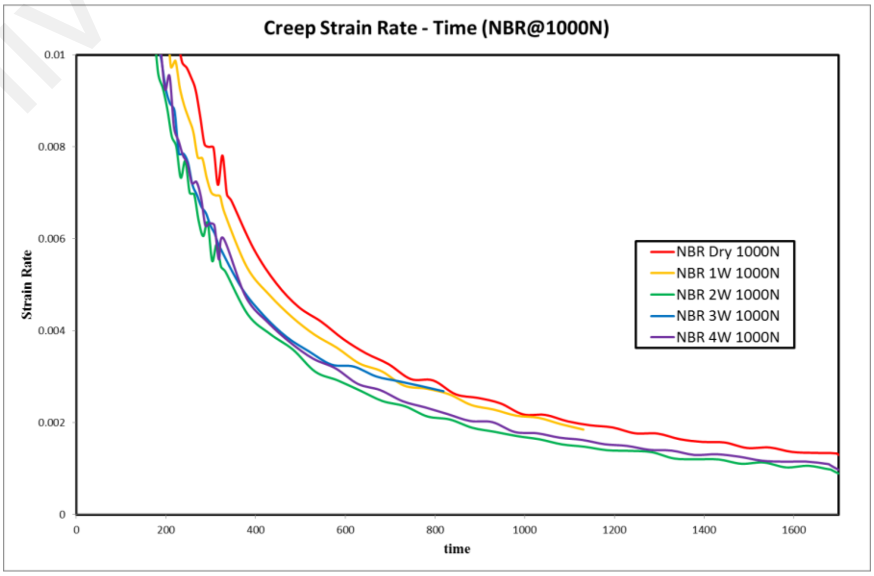
Creep Strain Rate - Time (NBR@1000N)
Strain Rate
0.01
0.008
0.006
0.004
0.002
0
0
200
400
600
800
1000
1200
1400
1600
time
NBR Dry 1000N
NBR 1W 1000N
NBR 2W 1000N
NBR 3W 1000N
NBR 4W 1000N

Appendix 6: Creep Strain Rate – Normalized Creep

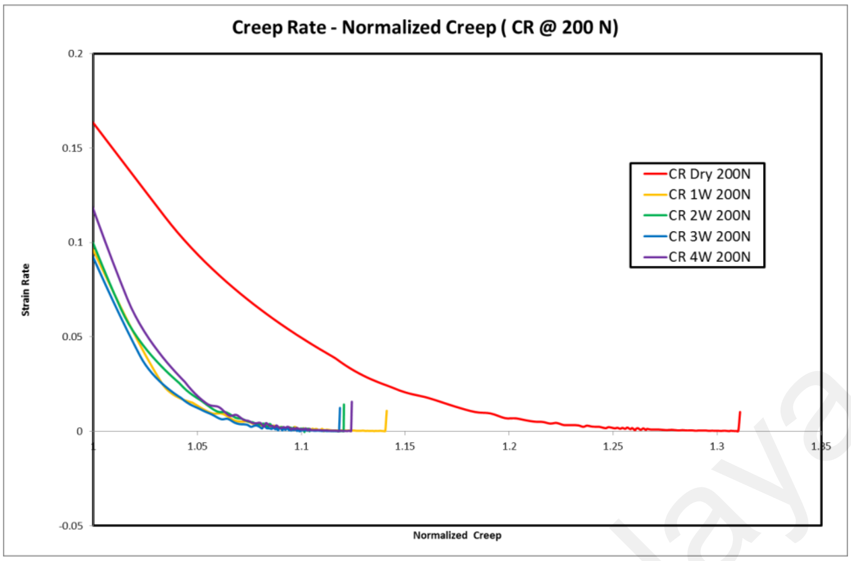

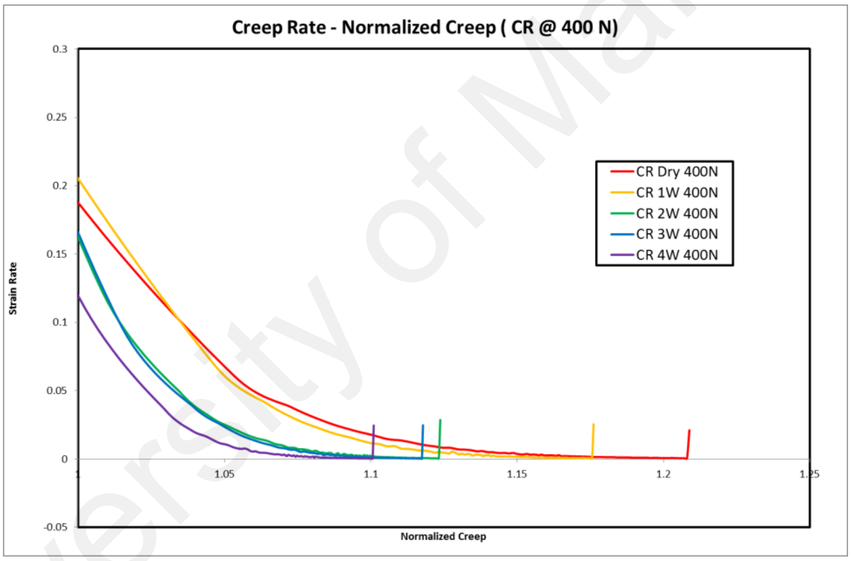

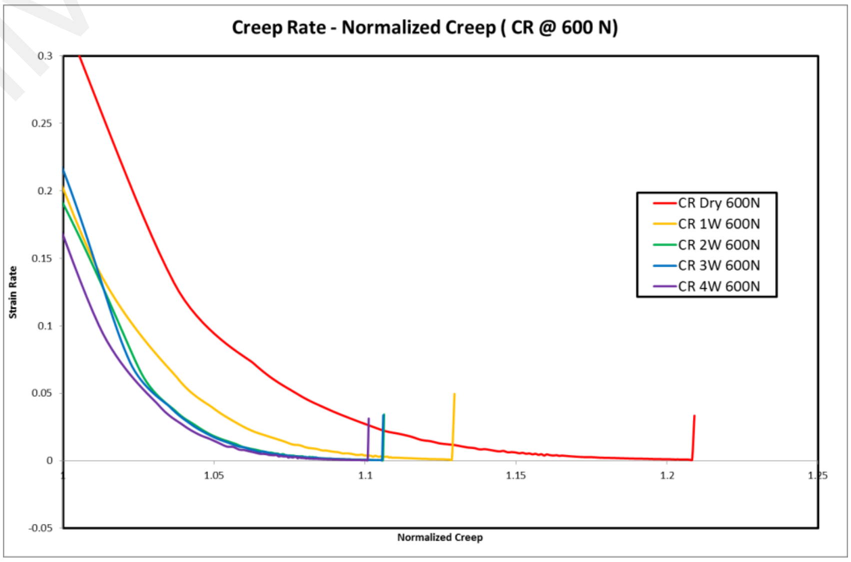

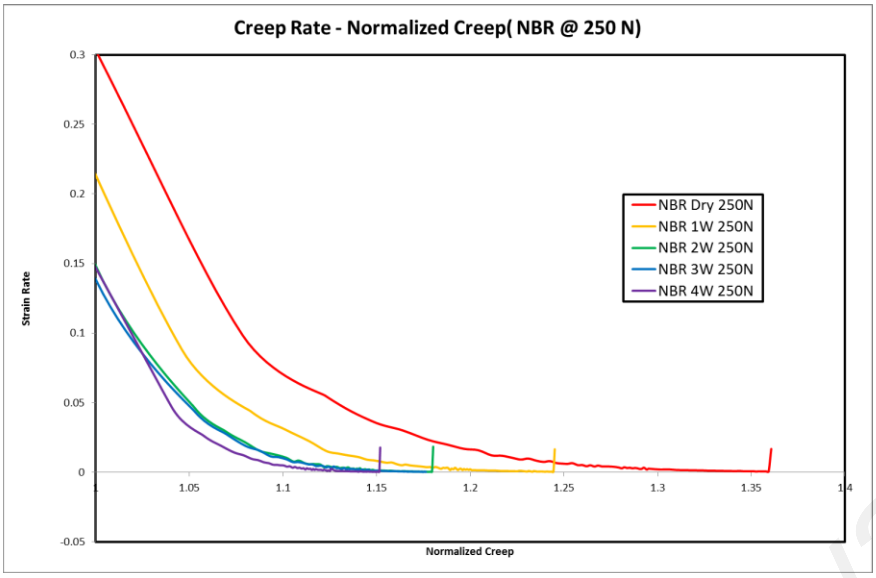
Creep Rate - Normalized Creep(NBR @ 250 N)
Strain Rate
0.3
0.25
0.2
0.15
0.1
0.05
0
-0.05
1
1.05
1.1
1.15
1.2
1.25
1.3
1.35
1.4
Normalized Creep
NBR Dry 250N
NBR 1W 250N
NBR 2W 250N
NBR 3W 250N
NBR 4W 250N

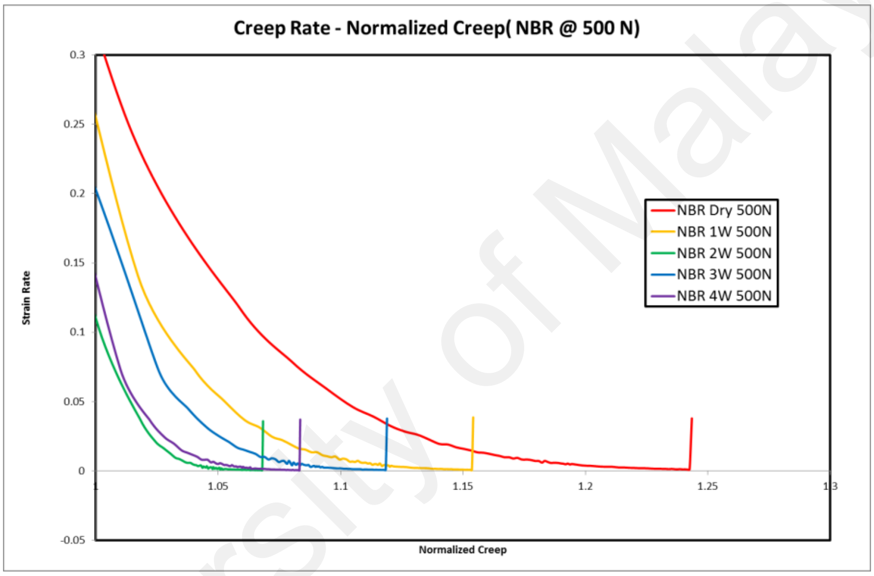
Creep Rate - Normalized Creep(NBR @ 500 N)
Strain Rate
0.3
0.25
0.2
0.15
0.1
0.05
0
-0.05
1
1.05
1.1
1.15
1.2
1.25
1.3
Normalized Creep
NBR Dry 500N
NBR 1W 500N
NBR 2W 500N
NBR 3W 500N
NBR 4W 500N

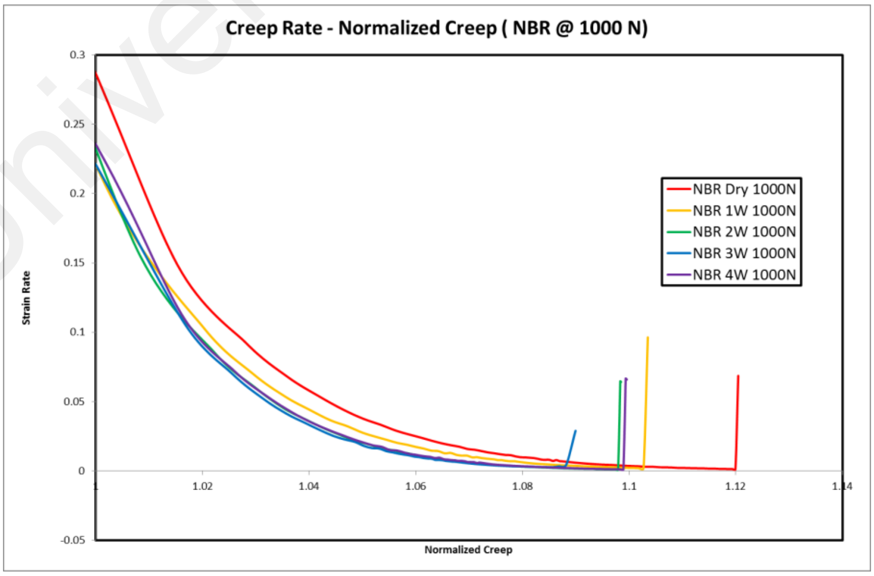
Creep Rate - Normalized Creep (NBR @ 1000 N)
Strain Rate
0.3
0.25
0.2
0.15
0.1
0.05
0
-0.05
1
1.02
1.04
1.06
1.08
1.1
1.12
1.14
Normalized Creep
NBR Dry 1000N
NBR 1W 1000N
NBR 2W 1000N
NBR 3W 1000N
NBR 4W 1000N